# Effect of Relocated Thermal and Pressure Stimuli on Vibrotactile Sensitivity

M.Sc. Robotics Thesis

Huibert A. J. van Riessen

Delft University of Technology

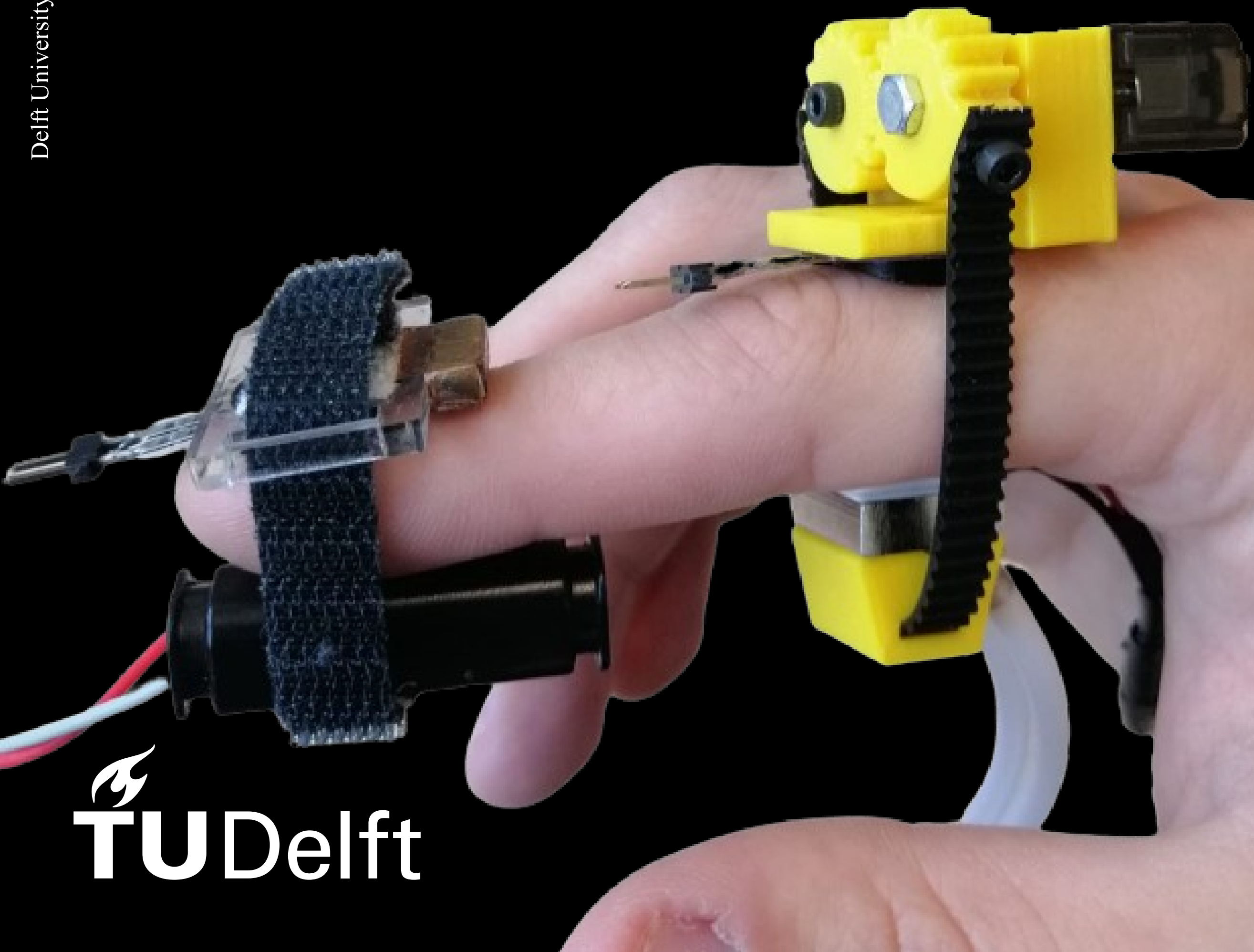

TU Delft

# Effect of Relocated Thermal and Pressure Stimuli on Vibrotactile Sensitivity

M.Sc. Robotics Thesis

by

Huibert A. J. van Riessen

to obtain the degree of Master of Science
at the Delft University of Technology,
to be defended publicly on Monday September 25, 2023 at 09:30 AM.

| | |
|---|---|
| Student number: | 5400163 |
| Supervisor: | Dr. Y. Vardar |
| Project Duration: | November, 2022 - September, 2023 |
| Faculty: | Cognitive Robotics |
| Thesis committee: | Dr. Y. Vardar, TU Delft, Chair |
| | Dr. Y. B. Eisma, TU Delft, External member |
| | Dr. D. Pool, TU Delft, External member |

TU Delft

# Acknowledgements

Pursuing a master's degree is not a one-person job. After working for three years in the industry, getting back into academics was quite a challenge. Still, I am grateful for this opportunity to learn more about my passion and meet incredible people. This exciting journey would not have been possible without the help and support of the people around me.

First, I would like to thank Yasemin Vardar for always believing in me. Not only did you supervise me during this second year of the Robotics master's, but you also inspired me to dream big and make the most out of this fantastic year. I felt comfortable sharing my highs and lows, and you were there to bring the best out of me. Our shared goal of making digital touch sensations feel real brought us together, and I believe our paths will cross again in the future to make this happen.

Furthermore, I would like to thank all members of HITLab for the fantastic discussions and good times. Specifically, Bence Kodak and Jagan Balasubramanian, your experience and supportive attitude helped tremendously during the design and experiment phases. Also, I had a great time supervising the internship of Beril Bildirici during the last three months of the project. Working with you was always fun; you grew so much during this period, and your excitement made our time together enjoyable.

Along the way, I made many new friends who made my time at TU Delft unforgettable. I cannot name all, but I would like to highlight Balazs, Emre, Luc, and Rogier. We did many projects together and spent countless hours hanging out both online and offline. My time on campus would not be the same without you.

Simone, my love, I don't have enough words to thank you. This journey has not always been easy, and coming home to you and our cat Pumpkin was always something to look forward to. You were always there for me, and I will always be there for you.

A final thank you to my parents, my sister Rosa, and her husband Kemal. Your unconditional love and support helped me thrive during this time, and I feel sincerely blessed that you are my family.

# Contents

**Acknowledgements** **i**

**1 Introduction** **1**

**2 Paper: Relocated thermal and pressure stimuli do not affect vibrotactile sensitivity on the fingertip** **2**

**A Multimodal Haptic Ring Design** **10**
A.1 Design process . . . . . 10
A.2 Calculations . . . . . 11
A.3 Technical drawings . . . . . 12

**B Stimuli parameters and measurements** **18**
B.1 Parameters . . . . . 18
B.2 Measurements . . . . . 19

**C Pseudo code** **20**

**D Additional data insights** **22**

**E Safety and Ethics** **24**
E.1 Device report . . . . . 24
E.2 Informed consent form . . . . . 30

**References** **32**

# 1 Introduction

This thesis is built around the paper ”Relocated thermal and pressure stimuli do not affect vibrotactile sensitivity on the fingertip”, which was carefully written to be published in a journal for papers around six pages. The paper includes an introduction section to mention problems, possible solutions, relevant literature, and the research question, a methods section describing every part related to the experiment, a results section to compare findings, and a discussion section to summarize all the findings and discuss results. Other information that did not fit the paper can be found in the appendices.

Appendix A summarizes the design process of the custom multimodal haptic ring used in experiments. This includes requirements, calculations, and technical drawings that helped to form the final design. The device was made from scratch without any previous reference from previous lab members. Appendix B reports the parameters used for the thermal and pressure stimuli and includes measurements for verification purposes. Appendix C shows the functionality of the vibrotactile sensitivity experiment. The code is initially written in Matlab, but here, it is translated to pseudo-code for easy understanding. Appendix D gives more information related to our results, with per-participant measurements and comparisons. It also goes over the effect of condition order to show how results fluctuate over time. Lastly, Appendix E incorporates sections of the Human Research Ethics Committee application to give insights into the design considerations to mitigate risks.

# 2

# Paper: Relocated thermal and pressure stimuli do not affect vibrotactile sensitivity on the fingertip

# Relocated thermal and pressure stimuli do not affect vibrotactile sensitivity on the fingertip

Huibert A. J. van Riessen and Yasemin Vardar

***Abstract*—Relocated haptic feedback from the fingertip to the proximal phalanx can alter the perception of physical interactions by simultaneously displaying relocated multi-modal tactile cues. However, how these relocated tactile cues alter the vibrotactile sensitivity of the fingertip remains unclear. This two-site stimulation study employs a custom-designed multimodal haptic ring for the proximal phalanx to evaluate the effect of relocated cold, hot, and pressure stimuli on the vibrotactile sensitivity of the fingertip. Our results show no significant difference between the vibratory detection thresholds of six multimodal tactile conditions. In contrast to single-site multimodal stimulation, where vibrotactile sensitivity is significantly altered by pressure and thermal stimuli, these results imply the feasibility of applying thermal and pressure stimuli without significantly altering fingertip sensitivity. Relocation of tactile stimuli keeps the vibrotactile sensitivity of the fingertip intact and opens up the possibility of altering tactile perception while interacting with the physical environment, making this technology feasible for mixed reality applications.**

***Index Terms*—Multisensory, Multimodal, Thermal, Pressure, Vibrotactile, Tactile perception, Mixed reality, Wearable**

## I. Introduction

TACTILE exploration gives us important information about our surroundings. Wearable haptic devices that display tactile modalities can mimic touch sensations in virtual environments, breaching the gap between the physical and digital realms. Many wearable haptic devices are designed to apply multimodal tactile stimuli to the fingertip [1] [2] [3]. However, directly mounting haptic devices to the fingertip causes limitations.

Occluding fingertips with wearable devices limits the range of motion since it adds thickness to the fingertip, which increases the likelihood of collisions and could result in the inability to perform tasks featuring small objects or confined spaces. Moreover, occluded fingertips prevent direct interaction with the physical environment, restricting interactions with tangible objects, which limits mixed reality applications [4]. Placing wearable devices directly on the fingertip also causes occlusions for hand tracking performed by computer vision algorithms [5]. These problems could be solved by relocating the tactile sensations to free the fingertip (see Fig. 1).

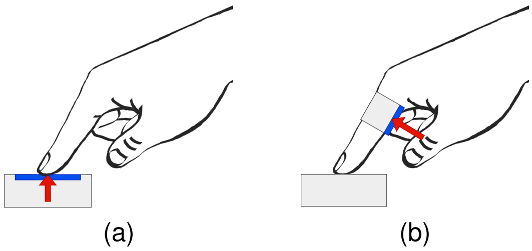


Fig. 1. (a) Pressure (red) and thermal (blue) stimuli perceived simultaneously by interacting with the material surface. (b) Relocated pressure (red) and thermal (blue) stimuli are applied to the proximal phalanx and simultaneously perceived during interaction with the material surface with the fingertip.

Previous works presented haptic devices that relocate tactile stimuli to prevent fingertip occlusions. Pachierotti et al. [5] proposed the "hRing" device, which uses two servo motors in combination with a belt for rendering pressure at the proximal phalanx of the index finger. They showed that relocated pressure stimuli can improve the performance of pick-and-place tasks while leaving the fingertip unobstructed. Gioioso et al. [6] introduced a wearable haptic ring that can apply thermal and pressure cues to the proximal phalanx. This haptic ring contains a Peltier cell for thermal stimuli, which is mounted on a moving platform for applying pressure stimuli. They developed a virtual reality application to show the feasibility of thermal discrimination, even though the thermal cues are not directly applied to the fingertip. Palmer et al. [7] showed multiple mappings for relocating forces from the thumb and index finger to the wrist and their benefits during pick-and-place tasks when visual feedback is limited. Pezent et al. [8] proposed "Tasbi", a wrist-worn device that combines vibrotactile and squeeze stimuli during augmented and virtual reality interactions, and showed multiple applications where these relocated tactile stimuli are combined with visual feedback to create visual pseudo-haptic illusions of tactile interactions [9]. Tanaka et al. [10] introduced a full-hand electro-tactile feedback system in which they attached electrodes to the wrist and the back of the

H.A.J. van Riessen and Y. Vardar are with the Department of Cognitive Robotics, Faculty of 3ME, Delft University of Technology, 2628 CD Delft, The Netherlands. E-mails: HvanRiessen@tudelft.nl, Y.Vardar@tudelft.nl.

hand to apply electro-tactile stimuli to the nerves while keeping the palmar side unobstructed. Their experiments showed that participants most dominantly localized the tactile sensations on the palmar side of the hand while they were actually applied to the dorsal side. Other studies demonstrated that relocating vibration stimuli on the proximal phalanx of the index finger [11] or wrist [12] can be utilized for displaying information, such as the texture of materials.

It has already been shown that relocated tactile cues can alter perceived physical properties. This was shown in previous research conducted by de Tinguy et al. [13], who utilized the earlier mentioned ”hRing” device to increase the perceived stiffness of tangible objects. Two years later, Salazar et al. [14] performed experiments showing that decreasing the perceived stiffness with relocated pressure stimuli is possible. Asano et al. [15] demonstrated that a vibrating voice-coil actuator worn on the side of the finger can modify the perceived roughness of physical objects. Moreover, Jamalzadeh et al. [16] showed that subthreshold vibrotactile stimuli applied on the proximal phalanx of the index finger increased the detection threshold of electrovibration stimuli perceived on the fingertip. The mentioned examples prove the feasibility of relocating tactile stimuli with a perceptual modality for altering a related perceived sensation of an object (e.g., remote pressure vs. perceived stiffness). However, it is unclear how tactile stimuli perceived on the fingertip would be affected by relocated tactile stimuli with a different modality.

Previous works investigated the interactions between stimuli with different modalities applied on the same skin site. For example, thermal stimuli, especially cold stimuli, have been shown to affect vibrotactile sensitivity in same-site stimulation studies. Weitz [17] showed that vibrotactile sensitivity is a U-shaped function of skin temperature featuring the forearm. Green [18] expanded this research by showing that at a vibration frequency of 250 Hz, skin sensitivity of the thenar eminance is highest at 34 °C, is lowered substantially by cooling the skin to 20 °C, while heating the skin to 42 °C caused a slight reduction in sensitivity. Sensitivity for 30 Hz vibrations also decreases for the mentioned skin temperatures, but significantly less, indicating that the independency of these tactile modalities varies for different vibration frequencies. Later, Klinenberg et al. [19] confirmed a similar relation between the significant reduction in fingertip vibrotactile sensitivity of 250 Hz vibrations caused by reducing the fingertip temperature to 17 °C.

Pressure stimuli also alter vibrotactile sensitivity in single-site stimulation studies, but the effects vary depending on the applied contact force and the vibration frequency. Pappeti et al. [20]. researched the effect of pressing forces on vibrotactile sensitivity with vibrations at 250 Hz, showing that vibration sensitivity increased significantly for pressing forces up to 7.6 N, followed by a slight sensitivity increase for 14.4 N. Later, Oh and Choi [21] did similar research for both 250 Hz and 40 Hz vibrations. They showed that detection thresholds at 40 Hz were higher than 250 Hz vibrations and confirmed that vibrotactile sensitivity increased at 250 Hz with increasing pressing forces up to 7.9 N.

Although thermal and pressure stimuli alter the perception of same-site vibrotactile stimuli, the effect of these relocated stimuli on vibrotactile sensitivity during two-site stimulation remains unclear. Reduced vibrotactile sensitivity limits the range of displayable roughness of digital textures, as perceptual roughness increases with the intensity of vibrations [22]. Moreover, reduced finger sensitivity caused by cold stimuli has been shown to affect performance during manual tasks [23]. Relocating thermal stimuli might prevent sensitivity reduction, which opens up their usage during remote robotic surgery or other high-demanding telerobotic applications. In this study, we designed a multimodal haptic ring that can apply thermal and pressure stimuli to the proximal phalanx (inspired from [6]) and conducted a vibrotactile sensitivity experiment to answer the following research question:

> *How do relocated thermal and pressure stimuli applied to the proximal phalanx affect the vibrotactile sensitivity of the fingertip?*

## II. Methods

### A. Participants

Twelve males and three females, all right-handed, between the ages of 21 and 32 (mean: 24.5, standard deviation: 2.7), participated in the experiments. None of them had injuries or neurological problems in their right hands. The experimental procedures were conducted in accordance with the Declaration of Helsinki and approved by the Human Research Ethics Committee of TU Delft with case number 3279. All participants gave informed consent.

### B. Experimental setup

During the experiments, a participant sat in front of a monitor displaying a graphical user interface (GUI) and a keyboard (Fig. 2a). They wore a custom-designed multimodal haptic device (Fig. 2b) displaying thermal and pressure stimuli to the proximal phalanx and vibrotactile stimuli on the fingerpad of the index finger of their right hand.

Our device delivers thermal stimuli via a $15\times15\times3.6$ mm Peltier module (QC-31-1.0-3.9AS, QuickCool) mounted on the ventral side of the proximal phalanx. The Peltier temperature is regulated via a

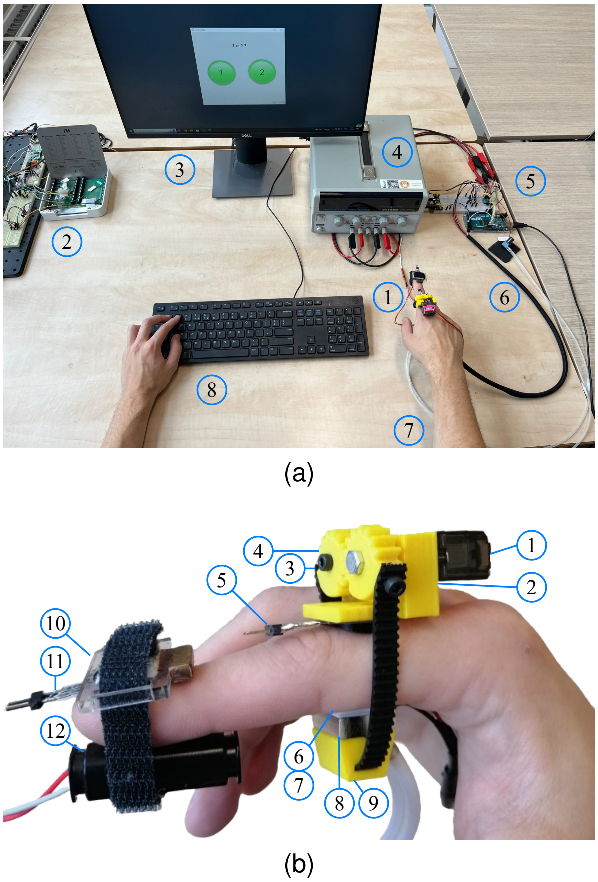


Fig. 2. (a) Experimental setup: 1. custom-designed multi-modal haptic device, 2. data acquisition board, 3. monitor displaying the GUI, 4. variable power supply, 5. Arduino, 6. water pump, 7. armrest, and 8. keyboard. (b) A closer look at the custom-designed haptic device: 1. servo motor, 2. servo motor housing, 3. servo belt, 4. spur gears, 5. force-resisting sensor, 6. NTC thermistor, 7. Peltier element, 8. water-cooling heat sink, 9. moving platform, 10. acrylic mounting plate, 11. force-sensing resistor, and 12. voice-coil actuator

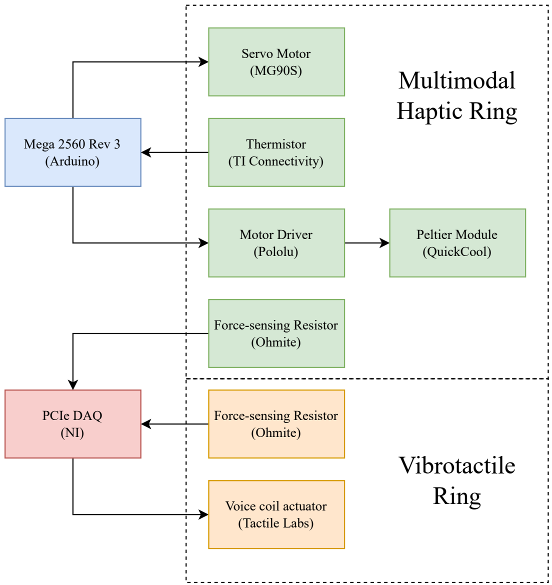


Fig. 3. Signal workflow showing the connections of hardware components of the multimodal haptic ring and the vibrotactile ring.

motor driver (DRV8833, Pololu) through a closed-loop PID controller by measuring temperature from a thermistor (GA10K3MCD1 NTC, TE Connectivity) placed between the skin and the Peltier module. The thermistor is connected to a microcontroller (Mega 2560 Rev 3, Arduino), which receives temperature data and handles the PID control of the Peltier module. This module sits on a water-cooled heat sink (MCX RAM, Alphacool), which is an effective method for regulating heat dissipation [24] [25]. A water pump (480-122, RS Pro) circulates the water through the heat sink with silicon hoses. The pump's input voltage was kept at 1.1 V throughout the entire experiment via a power supply (GPS-4303 DC Bench Power Supply, Gw Instek). Although fan cooling is also an option for regulating heat dissipation [6] [26], fans are substantially larger compared to water cooling elements, which could hinder the freedom of movement, and water cooling has no moving mechanical parts. This assembly is placed on the skin via a 3D-printed mount connected to a motor belt. The two ends of the belt are connected to 3D-printed spur gears for adjusting the strapping pressure. The spur gears move in opposite directions, moving the platform up or down, driven by an MG90S servo motor controlled by the microcontroller. The applied pressure is measured via a force sensor (FSR06B, Ohmite) mounted under the gears. The vibrotactile cues were delivered via a voice coil actuator (Haptuator Mark II, Tactile Labs) mounted on the fingertip via a velcro strap [11]. The signals for the actuator are generated via the data acquisition board and amplified by an audio amplifier (MIKROE-3077, Mikroe) with a 20 dB gain. The strapping force of the actuator is measured via a force sensor (FSR06B, Ohmite) mounted on the fingernail of the participant via the velcro strap, which sends force data to the data acquisition board.

The participant rested their forearm on an armrest (Model 332020, Ergorest) to prevent fatigue. They also wore noise-canceling headphones (WH-1000XM3, Sony) playing pink noise to prevent audio bias and for playing sound cues. They gave their answers with their left hand through the keyboard.

### C. Stimuli

In our experiments, the vibrotactile stimulus was a sinusoidal signal with a frequency of 250 Hz applied on the fingertip via the voice-coil actuator. We chose this frequency because it lies within the sensitive frequency region (between 150 and 300 Hz) for human perception of vibrotactile stimuli [27]. Also, it allowed us to compare our findings with previous literature that used the 250 Hz vibration frequency [18] [21]. The amplitude of the voice-coil actuator started at a high value (20 mV) and was adjusted during the experiments. The strapping force of the voice coil actuator was 0.5 N for all conditions to prevent setup slip from the hand during hand movements.

We tested the effect of three thermal and two pressure stimuli values on the vibrotactile sensitivity, resulting in six experimental conditions (see Table I). These were thermal stimuli of 40 °C (*hot*), 18 °C (*cold*), and 32 °C (*neutral*), accompanied by pressure stimuli of either 0.5 N (*low pressure*) or 2 N (*high pressure*). We selected these values to avoid the noxious response reported for temperatures below 15 °C and above 45 °C [28]. During the preliminary experiments, thermal stimuli below 18 °C and above 40 °C were perceived as painful by some participants; therefore, these values were selected as temperature limits. The pressure values were selected to keep functionality in mind, where the lowest pressure (0.5 N) corresponded to the strapping force, and 2 N was the highest pressure limit for comfort throughout one trial.

TABLE I
EXPERIMENTAL CONDITIONS

| Condition | Thermal | Pressure |
|---|---|---|
| Neutral - low pressure | 32 °C | 0.5 N |
| Neutral - high pressure | 32 °C | 2 N |
| Cold - low pressure | 18 °C | 0.5 N |
| Cold - high pressure | 18 °C | 2 N |
| Hot - low pressure | 40 °C | 0.5 N |
| Hot - high pressure | 40 °C | 2 N |

### D. Experimental procedure

Before the experiments, the participant washed their hands and used hand sanitizer. Then, the experimenter instructed the participant on how the experiment works. Afterward, the experimenter mounted the thermal and pressure module of the device to the participant's index finger and ensured that the mounting location was correct (see Fig. 2b). Then, the strapping force was increased by automatically adjusting the motor angle based on closed-loop force control until it reached the required pressure level. Then, the experimenter set the thermal condition until it reached the required temperature. Afterward, the experimenter mounted the vibrotactile module on the fingerpad of participant and manually adjusted the velcro strap until achieving a strapping force of 0.5 N. Then, the participant placed their forearm on the armrest and put on the noise-canceling headphones. After these procedures, the participant started the experiment without a training session by initiating the experiment by pressing the '2' key on the keyboard. Each participant conducted experiments with all conditions listed in Table I. They completed the experiments in different random order.

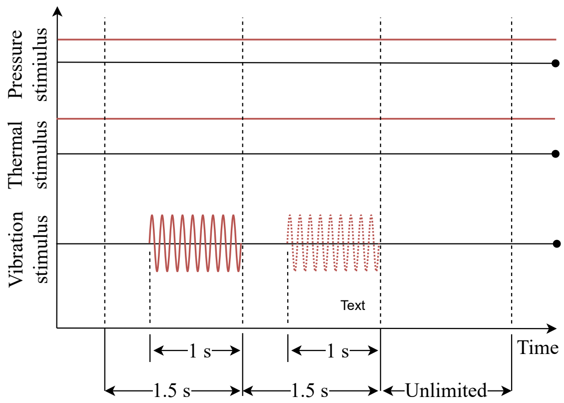


Fig. 4. Stimuli timing diagram for the vibrotactile sensitivity experiments. A sinusoidal vibrotactile stimulus (250 Hz) with a duration of 1 second was either present in the first or the second interval randomly. Pressure and thermal stimuli were always present during the trial and kept constant throughout all repetitions. The participant had to choose in which of these two intervals the vibrotactile stimulus was present.

We used a two-alternative-forced-choice method in our detection threshold experiments. The vibrotactile stimuli were presented with two temporal intervals signaled to the participants via the GUI as 1 and 2; only one of these intervals contained the test stimulus (see Fig. 4). The participant's task was to select the interval where they perceived a vibratory stimulus on their index fingertip. In each trial, the software randomized the interval during which the vibrotactile stimulus was present. Both pressure and thermal stimuli were always present during the entire session.

The participant was instructed to hold their index finger in the air and wait for a sound cue. Half a second later, the first interval played for 1 second. After that, the process was repeated for the second interval. After the second interval was completed, a different sound cue indicated it was time to select which of the two intervals contained the vibrotactile stimulus. The participant could answer by pressing the '1' or the '2' key on the keyboard, and they were indicated if their answer was correct or incorrect; see Fig. 4 for the stimuli timing diagram of the experiments.

The amplitude of the input voltage signal to the voice-coil actuator was modulated using a three-up/one-down adaptive staircase method (see Fig. 5). This method obtains thresholds with a correct response probability of 75% [29]. The staircase started with an easily perceivable

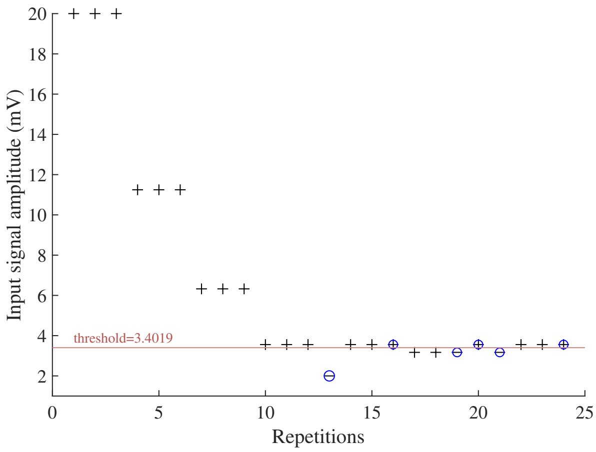


Fig. 5. An example session of the adaptive three-up/one-down staircase method [29]. The threshold value is calculated by averaging the last five reversals at the ±1 dB range. Correct answers are represented by plus signs (+), and minus signs (-) represent incorrect answers. The circles (o) show reversals, and the threshold is indicated with a red line.

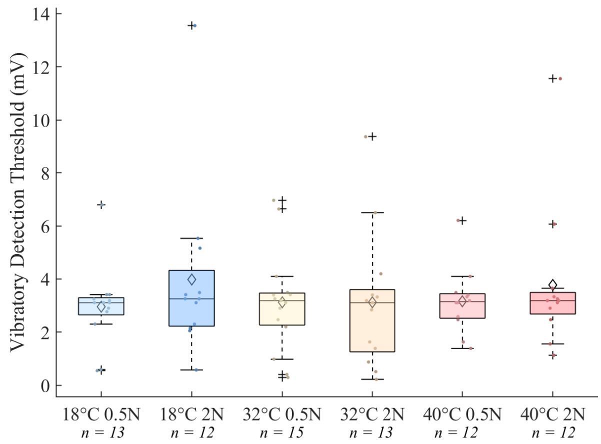


Fig. 6. Boxplots of the vibrotactile detection thresholds. The results corresponding to each experimental condition are color-coded. The center lines show the medians; box limits indicate the 25th and 75th percentiles. The whiskers extend to 1.5 times the interquartile range. Outliers are represented by plus signs (+), and diamonds (◇) represent sample means. The points (.) show individual threshold values; the sample sizes (*n*) are indicated under each boxplot.

magnitude (20 mV). After three correct answers (not necessarily consecutive), the vibrotactile signal amplitude was decreased by 5 dB increments at the start, and after one wrong answer, this increment was reduced to 1 dB. When participants gave one wrong answer, the amplitude was increased by 1 dB. One complete trial was finished when the last five reversals remained in the ±1 dB range, after which the mean of those five reversals revealed the detection threshold. Alternatively, to ensure participants' comfort, the trial stopped after 80 repetitions. When the session finished, the GUI indicated this, and a 10-minute resting period started. After six sessions (3 thermal × 2 pressure conditions), the experiment ended, resulting in a maximum duration of 2 hours.

## III. Results

The measured detection thresholds per condition are visualized in Fig. 6. The sessions in which the experiment was stopped due to reaching the maximum amount of repetitions (80) were excluded from the data analysis.

First, we applied Shapiro-Wilk tests [30] to each distribution to check whether they distributed normally. For neutral-low pressure (Mean: 3.12, SD: 1.88), neutral-high pressure (Mean: 3.12, SD: 2.54), and hot-low pressure (Mean: 3.17, SD: 1.23) conditions, the Shapiro-Wilk test suggested that they follow a normal distribution ($p > 0.05$). However, it indicated that cold-low pressure (Mean: 2.96, SD: 1.50), cold-high pressure (Mean: 3.99, SD: 3.29) and hot-high pressure (Mean: 3.78, SD: 2.73) conditions are not normally distributed ($p < 0.05$).

As not all data is normally distributed, we applied a two-way non-parametric Skillings-Mack test [31], suitable as an alternative to the Friedman test when data contains missing entries, to analyze the effects of relocated thermal and pressure stimuli on vibrotactile sensitivity on the fingertip. We evaluated the effect of relocated thermal stimuli by taking three thermal conditions as treatments and two pressure conditions as blocks. Our results showed that relocated thermal stimuli did not significantly affect the vibratory detection thresholds ($T(2) = 0.23$, $p = 0.893$). Similarly, we evaluated the effect of relocated pressure by taking two pressure conditions as treatments and three thermal conditions as blocks. Our results showed that relocated pressure stimuli did not significantly affect the vibratory detection thresholds ($T(1) = 0.14$, $p = 0.7106$).

## IV. Discussion

In this study, we evaluated the effect of relocated thermal and pressure stimuli on the vibrotactile sensitivity of the fingertip. We first designed a custom haptic device that applied thermal and pressure stimuli to the proximal phalanx and vibrotactile stimuli on the index fingertip. Then, we measured the detection thresholds of 15 participants for 250 Hz vibration stimuli for six thermal and pressure conditions.

Our results showed no significant effect of relocated thermal stimuli on vibratory detection thresholds measured on the fingertip (see Fig. 6). This finding differs from the previous works, which tested the effect of thermal stimuli on the vibrotactile sensitivity on the *same* skin site. Those works reported a consistent reduction in sensitivity to 250Hz vibration with hot [17] [18] and especially cold stimuli [32] [19]. These results were explained with the temperature-dependent sensitivity of Pacinian corpuscles, which are responsible for detecting 250 Hz vibrations [18]. This situation could explain why there was no consistent vibrotactile sensitivity reduction based on relocated thermal stimuli in our study, as our device did not directly apply thermal stimuli near the mechanoreceptors of the fingertip. It is also possible that thermal and vibrotactile stimuli are processed independently [33] and do not affect each other when applied at different skin locations. Interestingly, in our study, participants stated that they felt thermal stimuli most intense during initial calibration. This phenomenon is called thermal adaptation, where participants become less responsive to thermal stimuli due to continuous exposure over time [28]. Thus, focusing on the vibrotactile stimuli becomes less demanding when the repetition number rises during thermal conditions. In our future work, we plan to repeat the same experiments by initializing the thermal stimulus in each trial.

The results indicate that relocated pressure stimuli do not significantly affect vibrotactile sensitivity on another site. This result contradicts the previous single-site studies, which showed that increasing contact force increases sensitivity to 250 Hz vibration stimuli applied at the *same* skin site [21] [20]. Pacinian corpuscles lie in deeper layers of the skin, and the transmission of vibrations increases when the skin is compressed [21], causing higher vibration sensitivity. As the pressure applied by our haptic device is located at the proximal phalanx and not at the source of the vibration, this might act as a distraction instead of more effectively transmitting vibrations. This distraction may be the reason for the higher standard deviations and outliers, as all maximum threshold values occurred in high pressure conditions. Moreover, previous research has shown that the perceived intensity of tactile stimuli applied to the fingertip decreases exponentially over time [34]. This tactile adaptation might have made the pressure sensation less distracting over time, leading to a reduced perceptual difference between high and low pressure conditions, ultimately resulting in comparable threshold outcomes for both conditions.

We observed large variabilities between participant responses. For example, participant 4, who had the lowest thresholds of any participant, could only converge for neutral temperatures. For this participant, thermal conditions caused too much distraction, resulting in the inability to finish the experiment within 80 repetitions. In contrast, participant 10 had the highest overall thresholds for all conditions; however they were affected more by pressure than other participants, showing a substantial difference between low and high pressure conditions. Participant 3 had issues with converging for the hot conditions, while they found cold ones refreshing. Previous work also mentions this high degree of variation in perception of vibrotactile, thermal, and pressure stimuli [35]. They state that not only personal qualities cause variability but also distraction, motivation, fatigue, and anxiety due to testing participants' abilities. However, this variability is most influential when studying individual participants and has less effect on the overall comparison between condition groups.

Despite carefully designed experimental setup and procedures, our work had several limitations that could affected our results. For example, the selected temperature and pressure levels were conservative and within comfortable ranges. More extreme values just above the pain threshold could alter the vibrotactile sensitivity. Moreover, device ergonomics limited applied pressure ranges. Attachment forces lower than 0.5 N caused the haptic device to slip when moving around. Adding an external mount could prevent this slippage and open up the possibility of reducing the attachment force even further. However, this addition introduces a second pressure point to the assembly, which is why it was excluded from the current design.

In future studies, this technology can be utilized for mixed-reality applications, where relocated tactile cues can be combined with visual stimuli to alter the perception of tangible objects [2], enabling a crossover between physical and digital tactile interactions. Furthermore, relocated pressure and thermal stimuli have the potential to facilitate information transfer in precise telerobotics applications where it is crucial to maintain finger sensitivity, such as surgical tasks. Both vibrotactile and thermal stimuli are feasible for information transfer [33], and we showed that by relocating the thermal stimuli, the vibrotactile intensity range is not significantly altered. Moreover, tactile stimuli at the fingertip with simultaneous remote thermal stimuli can induce thermal referral [36], creating the illusion of thermal sensations at the site of tactile stimulation. In addition, utilizing relocated pressure stimuli can create pseudo-haptic effects, such as increasing pressure during virtual button presses to simulate tactile feedback or introducing macro roughness bumps to recreate bumpy materials [9]. Combining these relocated tactile stimuli can create compelling tactile illusions while still being able to interact with the physical world around you.

## Acknowledgments

The authors thank Bence Kodak and Jagan K. Balasubramanian for their insights and suggestions, Jacques Brenkman and Maurits Pfaff for their advice on the experimental setup.

# REFERENCES


[1] M. Gabardi, M. Solazzi, D. Leonardis, and A. Frisoli, “A new wearable fingertip haptic interface for the rendering of virtual shapes and surface features,” in *2016 IEEE Haptics Symposium (HAPTICS)*. IEEE, 2016, pp. 140–146.

[2] T. Murakami, T. Person, C. L. Fernando, and K. Minamizawa, “Altered touch: miniature haptic display with force, thermal and tactile feedback for augmented haptics,” in *ACM SIGGRAPH 2017 Posters*, 2017, pp. 1–2.

[3] G. Spagnoletti, L. Meli, T. L. Baldi, G. Gioioso, C. Pacchierotti, and D. Prattichizzo, “Rendering of pressure and textures using wearable haptics in immersive vr environments,” in *2018 IEEE Conference on Virtual Reality and 3D User Interfaces (VR)*. IEEE, 2018, pp. 691–692.

[4] S.-Y. Teng and P. Lopes, “Xr needs” mixed feelings” engineering haptic devices that work in both virtual and physical realities,” *XRDS: Crossroads, The ACM Magazine for Students*, vol. 29, no. 1, pp. 44–47, 2022.

[5] C. Pacchierotti, G. Salvietti, I. Hussain, L. Meli, and D. Prattichizzo, “The hring: A wearable haptic device to avoid occlusions in hand tracking,” in *2016 IEEE Haptics Symposium (HAPTICS)*. IEEE, 2016, pp. 134–139.

[6] G. Gioioso, M. Pozzi, M. Aurilio, B. Peccerillo, G. Spagnoletti, and D. Prattichizzo, “Using wearable haptics for thermal discrimination in virtual reality scenarios,” in *International AsiaHaptics conference*. Springer, 2018, pp. 144–148.

[7] J. E. Palmer, M. Sarac, A. A. Garza, and A. M. Okamura, “Haptic feedback relocation from the fingertips to the wrist for two-finger manipulation in virtual reality,” in *2022 IEEE/RSJ International Conference on Intelligent Robots and Systems (IROS)*. IEEE, 2022, pp. 628–633.

[8] E. Pezent, A. Gupta, H. Duhaime, M. O’Malley, A. Israr, M. Samad, S. Robinson, P. Agarwal, H. Benko, and N. Colonnese, “Explorations of wrist haptic feedback for ar/vr interactions with tasbi,” in *Adjunct Proceedings of the 35th Annual ACM Symposium on User Interface Software and Technology*, 2022, pp. 1–5.

[9] E. Pezent, A. Macklin, J. M. Yau, N. Colonnese, and M. K. O’Malley, “Multisensory pseudo-haptics for rendering manual interactions with virtual objects,” *Advanced Intelligent Systems*, p. 2200303, 2023.

[10] Y. Tanaka, A. Shen, A. Kong, and P. Lopes, “Full-hand electro-tactile feedback without obstructing palmar side of hand,” in *Proceedings of the 2023 CHI Conference on Human Factors in Computing Systems*, 2023, pp. 1–15.

[11] R. F. Friesen and Y. Vardar, “Perceived realism of virtual textures rendered by a vibrotactile wearable ring display,” *IEEE Transactions on Haptics*, 2023.

[12] C. Gaudeni, L. Meli, L. Jones, and D. Prattichizzo, “Presenting surface features using a haptic ring: A psychophysical study on relocating vibrotactile feedback,” *IEEE Transactions on Haptics*, vol. 12, no. 4, pp. 428–437, 2019.

[13] X. De Tinguy, C. Pacchierotti, M. Marchal, and A. Lécuyer, “Enhancing the stiffness perception of tangible objects in mixed reality using wearable haptics,” in *2018 IEEE Conference on Virtual Reality and 3D User Interfaces (VR)*. IEEE, 2018, pp. 81–90.

[14] S. V. Salazar, C. Pacchierotti, X. de Tinguy, A. Maciel, and M. Marchal, “Altering the stiffness, friction, and shape perception of tangible objects in virtual reality using wearable haptics,” *IEEE transactions on haptics*, vol. 13, no. 1, pp. 167–174, 2020.

[15] S. Asano, S. Okamoto, and Y. Yamada, “Vibrotactile stimulation to increase and decrease texture roughness,” *IEEE Transactions on Human-Machine Systems*, vol. 45, no. 3, pp. 393–398, 2014.

[16] M. Jamalzadeh, B. Güçlü, Y. Vardar, and C. Basdogan, “Effect of remote masking on detection of electrovibration,” in *2019 IEEE World Haptics Conference (WHC)*. IEEE, 2019, pp. 229–234.

[17] J. Weitz, “Vibratory sensitivity as a function of skin temperature.” *Journal of experimental Psychology*, vol. 28, no. 1, p. 21, 1941.

[18] B. G. Green, “The effect of skin temperature on vibrotactile sensitivity,” *Perception & Psychophysics*, vol. 21, no. 3, pp. 243–248, 1977.

[19] E. Klinenberg, Y. So, and D. Rempel, “Temperature effects on vibrotactile sensitivity threshold measurements: implications for carpal tunnel screening tests,” *The Journal of hand surgery*, vol. 21, no. 1, pp. 132–137, 1996.

[20] S. Papetti, H. Järveläinen, B. L. Giordano, S. Schiesser, and M. Fröhlich, “Vibrotactile sensitivity in active touch: effect of pressing force,” *IEEE transactions on haptics*, vol. 10, no. 1, pp. 113–122, 2016.

[21] S. Oh and S. Choi, “Effects of contact force and vibration frequency on vibrotactile sensitivity during active touch,” *IEEE Transactions on Haptics*, vol. 12, no. 4, pp. 645–651, 2019.

[22] T. Yoshioka, S. J. Bensmaia, J. C. Craig, and S. S. Hsiao, “Texture perception through direct and indirect touch: An analysis of perceptual space for tactile textures in two modes of exploration,” *Somatosensory & motor research*, vol. 24, no. 1-2, pp. 53–70, 2007.

[23] J. M. Lockhart, H. O. Kiess, and T. J. Clegg, “Effect of rate and level of lowered finger surface temperature on manual performance.” *Journal of Applied Psychology*, vol. 60, no. 1, p. 106, 1975.

[24] M. Gabardi, D. Leonardis, M. Solazzi, and A. Frisoli, “Development of a miniaturized thermal module designed for integration in a wearable haptic device,” in *2018 IEEE Haptics Symposium (HAPTICS)*. IEEE, 2018, pp. 100–105.

[25] B. L. Kodak and Y. Vardar, “Feelpen: A haptic stylus displaying multimodal texture feels on touchscreens,” *IEEE/ASME Transactions on Mechatronics*, 2023.

[26] L. Peters, G. Serhat, and Y. Vardar, “Thermosurf: Thermal display technology for dynamic and multi-finger interactions,” *Ieee Access*, vol. 11, pp. 12 004–12 014, 2023.

[27] L. A. Jones and N. B. Sarter, “Tactile displays: Guidance for their design and application,” *Human factors*, vol. 50, no. 1, pp. 90–111, 2008.

[28] H.-N. Ho, “Material recognition based on thermal cues: Mechanisms and applications,” *Temperature*, vol. 5, no. 1, pp. 36–55, 2018.

[29] J. J. Zwislocki and E. M. Relkin, “On a psychophysical transformed-rule up and down method converging on a 75% level of correct responses,” *Proceedings of the National Academy of Sciences*, vol. 98, no. 8, pp. 4811–4814, 2001.

[30] A. BenSaïda. (2023) Shapiro-wilk and shapiro-francia normality tests. MATLAB Central File Exchange. [Online]. Available: https://www.mathworks.com/matlabcentral/fileexchange/13964-shapiro-wilk-and-shapiro-francia-normality-tests

[31] J. H. Skillings and G. A. Mack, “On the use of a friedman-type statistic in balanced and unbalanced block designs,” *Technometrics*, vol. 23, no. 2, pp. 171–177, 1981.

[32] R. T. Verrillo and S. J. Bolanowski Jr, “The effects of skin temperature on the psychophysical responses to vibration on glabrous and hairy skin,” *The Journal of the Acoustical Society of America*, vol. 80, no. 2, pp. 528–532, 1986.

[33] J. Park, J. Kim, C. Park, S. Oh, J. Park, and S. Choi, “A preliminary study on the perceptual independence between vibrotactile and thermal senses,” in *International Conference on Human Haptic Sensing and Touch Enabled Computer Applications*. Springer, 2022, pp. 75–83.

[34] S.-P. Kim, Y. G. Chung, S. W. Han, H.-S. Kim, S.-C. Chung, J.-Y. Park, and C. Wallraven, “Adaptation of cortical activity to sustained pressure stimulation on the fingertip,” *BMC Neuroscience*, 2015.

[35] J. Fagius and L. K. Wahren, “Variability of sensory threshold determination in clinical use,” *Journal of the neurological sciences*, vol. 51, no. 1, pp. 11–27, 1981.

[36] H.-N. Ho, J. Watanabe, H. Ando, and M. Kashino, “Mechanisms underlying referral of thermal sensations to sites of tactile stimulation,” *Journal of Neuroscience*, vol. 31, no. 1, pp. 208–213, 2011.

# A

# Multimodal Haptic Ring Design

## A.1. Design process

We specifically designed the multimodal haptic ring to use only one servo motor for applying pressure to limit the weight of the haptic ring. Our conditions only incorporate normal pressure stimuli, which can be achieved with one degree of freedom. Therefore, connected spur gears rotate oppositely to move the platform up and down. The driving spur gear contains a counterbore hole so the servo motor axis can fit around it, ensuring that the spur gear aligns perfectly with the driven gear. This driving spur gear is fixed to the motor axis by using a spring washer to battle loosening by motor vibrations. Both spur gears are rounded off on the belt side to ensure that the belt wraps smoothly around it during actuation. The holes in the gears have flattened top sides for mounting the bolts. The linear range of the platform is based on the diameter of the spur gears and the 180 °rotation of the servo motor. A custom-designed motor housing holds the servo motor in place and incorporates a sliding bearing for the driven spur gear. As the linear actuation should align with the force-sensing resistor (FSR), the housing contains an extended platform to center the FSR. The FSR has its own adhesive layer, which mounts it on the extended platform.

A Peltier element was chosen for thermal stimuli as it has a hot and a cold side. These sides can switch by changing the direction of the current. This approach has a downside: the cold side cannot maintain low temperatures without heat dissipation on the hot side due to heat transfer between sides. Therefore, a water heat sink transfers heat or cold from the opposing side. The heat sink mounts on the Peltier by using thermal conductive tape. Similarly, the thermistor is attached to the top side of the Peltier with thermal conductive tape. The overall size is selected to fit between most adult fingers without the edges sticking out. A custom-made housing is made for the heat sink, which is tightly dimensioned and makes the thermal module move vertically. This mount ensures the pressure is in line with the moving platform, but tolerances allow the platform to move alongside the belt for slight adjustments based on the user's finger.

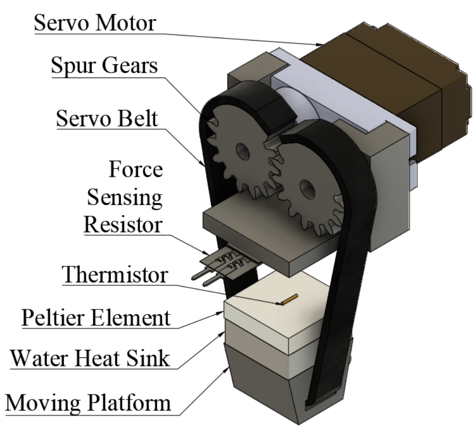


**Figure A.1:** Design and components of multimodal haptic ring.

**Table A.1:** Design requirements

| Description | Design requirement | Final design |
|---|---|---|
| Overall width dimension | < 40 mm | 36 mm |
| Weight | < 50 g | 43 g |
| *Thermal display* | | |
| Platform dimensions | 15 x 15 mm | 15 x 15 mm |
| Thickness | < 5 mm | 3.6 mm |
| Temperature range | 15 to 45 °C ($\Delta T = 30K$) | $\Delta T = 71K$ |
| Power peak | 4.2 W | 8.8 W |
| *Thermal measurement* | | |
| Thickness | < 1 mm | 0.5 mm |
| Temperature range | 5 to 55 °C | -40 to 125 °C |
| Resistance | - | 10kΩ |
| Response time | - | 200 ms |
| *Water cooling* | | |
| Hose diameter | 3 mm | 3 mm |
| Flow rate | 400 mL/min | 650 mL/min |
| Supply voltage | - | 1 -> 4 V |
| *Pressure display* | | |
| Voltage | 5 V | 4.8 - 6.0 V |
| Force | > 0.5 kg | 2.4 kg |
| Range | 20±5 mm | 13 - 25 mm |
| *Pressure measurement* | | |
| Sensor diameter size | < 20 mm | 18 mm |
| Actuation force | < 30 g | < 15 g |
| Load capacity | 2.4 kg | 5 kg |

## A.2. Calculations

The gear ratio must be considered when calculating the required force.

$$GR = n_{driven}/n_{driving} \tag{A.1}$$

Here, $GR$ is the gear ratio, $n_{driven}$ is the number of teeth of the driven gear, and $n_{driving}$ is the number of teeth for the gear directly connected to the motor. In our case, as both sides of the belt should move equally, the gear ratio should be 1. Both gears should have 15 teeth in this case.

The motor selection depends on availability, dimensions, weight, torque, and speed. Initial testing was performed with the MG90S, which is comparable with its larger brother, the MG90, but it trades some torque for speed. The torque of this motor is 1.8 kg/cm. The force that can be pulled using this torque depends on the radius of the pitch diameter of the spur gears:

$$F = \frac{\tau}{r} \tag{A.2}$$

Here, F is the force, $\tau$ is the torque, and r is the radius. In our case, the pitch diameter of 15 mm results in a radius of 0.75 cm. So, our setup can apply pressure of approximately $F = \frac{\tau}{r} = \frac{1.8}{0.75} = 2.4kg$ when a rope is connected to both spur gears.

To select the Peltier module, a similar approach as mentioned in [1] is used to calculate the required heat power based on the size of the Peltier. For this, we need to know what the thermal response is when the skin touches the Peltier surface. The following formula estimates the instant heat flux generated by the contact between the skin and the object [2]:

$$q\text{"}(t) = \frac{T_{skin}(t) - T_{object}(t)}{R_{skin-object}} \tag{A.3}$$

Here, $q"(t)$ is the instant heat flux between skin and object, $T_{skin}(t)$ is the skin temperature, $T_{object}(t)$ is the temperature of the Peltier surface, $R_{skin-object}$ is the thermal contact resistance and $t$ is the time. As our high pressure condition is 2N, the following model can be used to obtain a numerical approximate for the thermal contact resistance [3]:

$$R_{skin-object} = \frac{0.37 + k_{object}}{1870 * k_{object}} \tag{A.4}$$

Here, $k_{object}$ is defined as the object's thermal conductivity. To simulate the worst-case scenario, copper is selected due to its high thermal conductivity ($k_{copper} = 401W/mK$). This results in a thermal contact resistance of $Rskin - copper = 5.35 \times 10^{-4} m^2K/W$. Throughout the experiment, the neutral skin temperature is assumed to be 32 °C, and 22 °C is assumed as Peltier starting temperature, resulting in a maximum value of $q" = 18.68kW/m^2$. As the complete Peltier module touches the skin, the surface is $15 \times 15 = 225mm^2$, and thus, the Peltier has to be able to supply a heat pump power peak of $Q_{max} = 4.2W$. Our selected Peltier has a $Q_{max} = 8.8W$, which gives space to the required current needed and helps keep more options open for selecting the Peltier motor driver.

As the heat power peak is $Q_{max} = 8.8W$, the water flow must be sufficient to cool this down. For this, the rewritten formula for heat transfer can be used:

$$\dot{m} = \frac{Q}{C_p * \Delta T} \tag{A.5}$$

Here, $\dot{m}$ is the mass flow rate of water, $C_p$ is the specific heat capacity of water, Q is the heat radiated by the Peltier module, and $\Delta T$ is the difference between the hot and cold sides. To assume a worst-case scenario, take the maximum $\Delta T = 30K$. We take $C_p = 4,186kj/kg - K$ for water, resulting in $\dot{m} = 397.8mL/min$. The pump we chose has a maximum capacity of $650mL/min$, which leaves room to change the pump's voltage, which changes the flow rate.

## A.3. Technical drawings

As all the custom parts are 3D printed in PLA, the following drawings are included for checking the overall dimensions and layering.

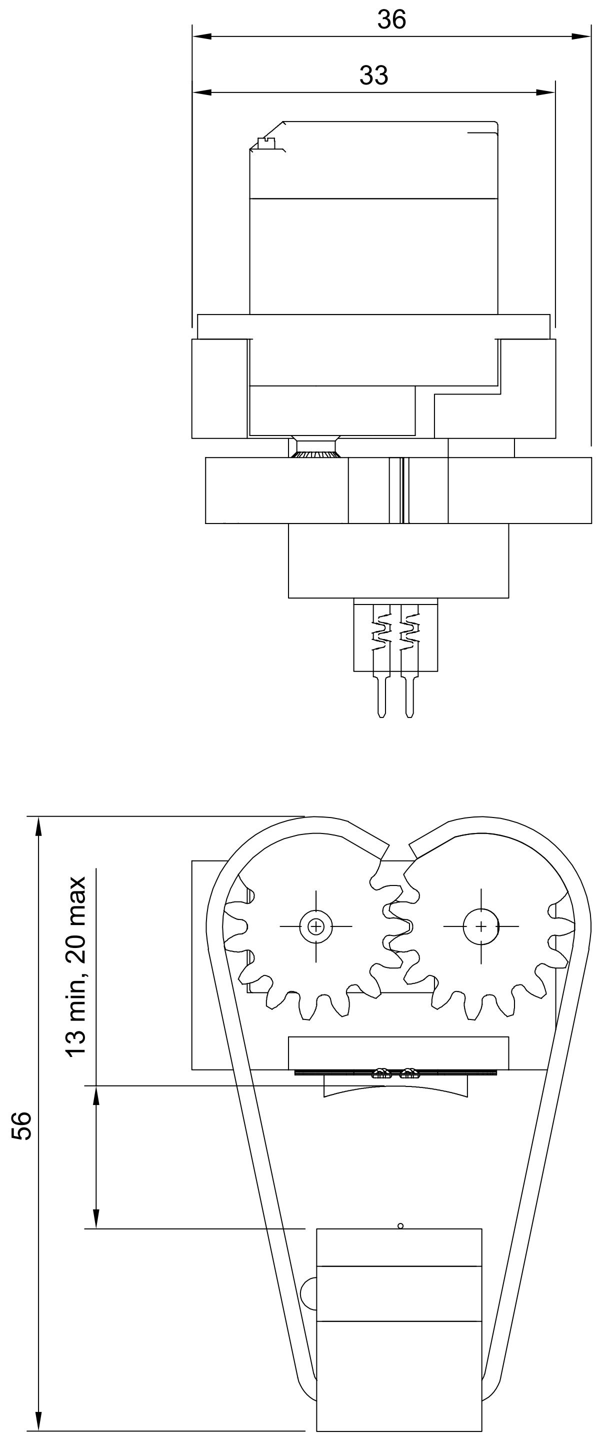


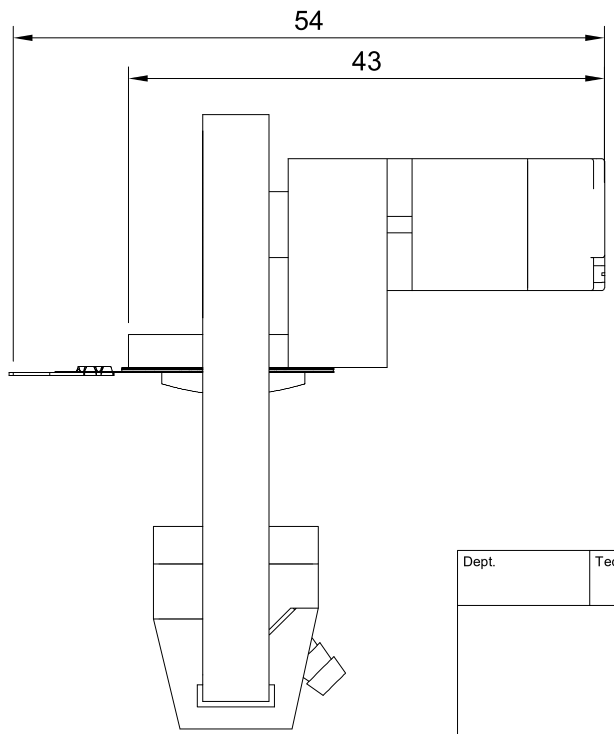


| Parts List | | | |
|---|---|---|---|
| Item | Qty | Part Number | Description |
| 1 | 1 | MountingPlate-15teeth-spur | |
| 2 | 1 | MG90S | |
| 3 | 1 | Spur Gear (15 teeth) | Spur Gear; Module: 1.0; Num Teeth: 15; Pressure Angle: 20.0; Backlash: 0.15 mm |
| 4 | 1 | Spur Gear (15 teeth) (1) | Spur Gear; Module: 1.0; Num Teeth: 15; Pressure Angle: 20.0; Backlash: 0.15 mm |
| 5 | 1 | 30-00016-FSR 402 Short Tail | |
| 6 | 1 | MCX RAM | |
| 7 | 1 | MCXMountv1 | |
| 8 | 1 | Component11 | |
| 10 | 1 | Component13 | |
| 11 | 1 | Curvedplate | |

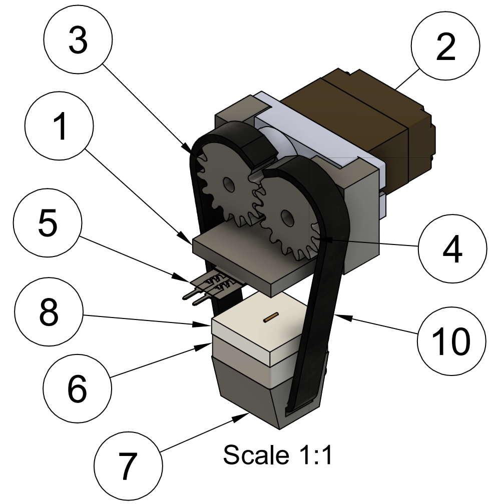

Scale 1:1

| Dept. | Technical reference | Created by<br>Bram Van Riessen 01/09/2023 | Approved by | | |
|---|---|---|---|---|---|
| | | Document type<br>A3 | Document status | | |
| | | Title<br>AssemblyMG90S-15teeth-spur<br>Scale 2:1 | DWG No. | | |
| | | | Rev. | Date of issue | Sheet<br>1/1 |

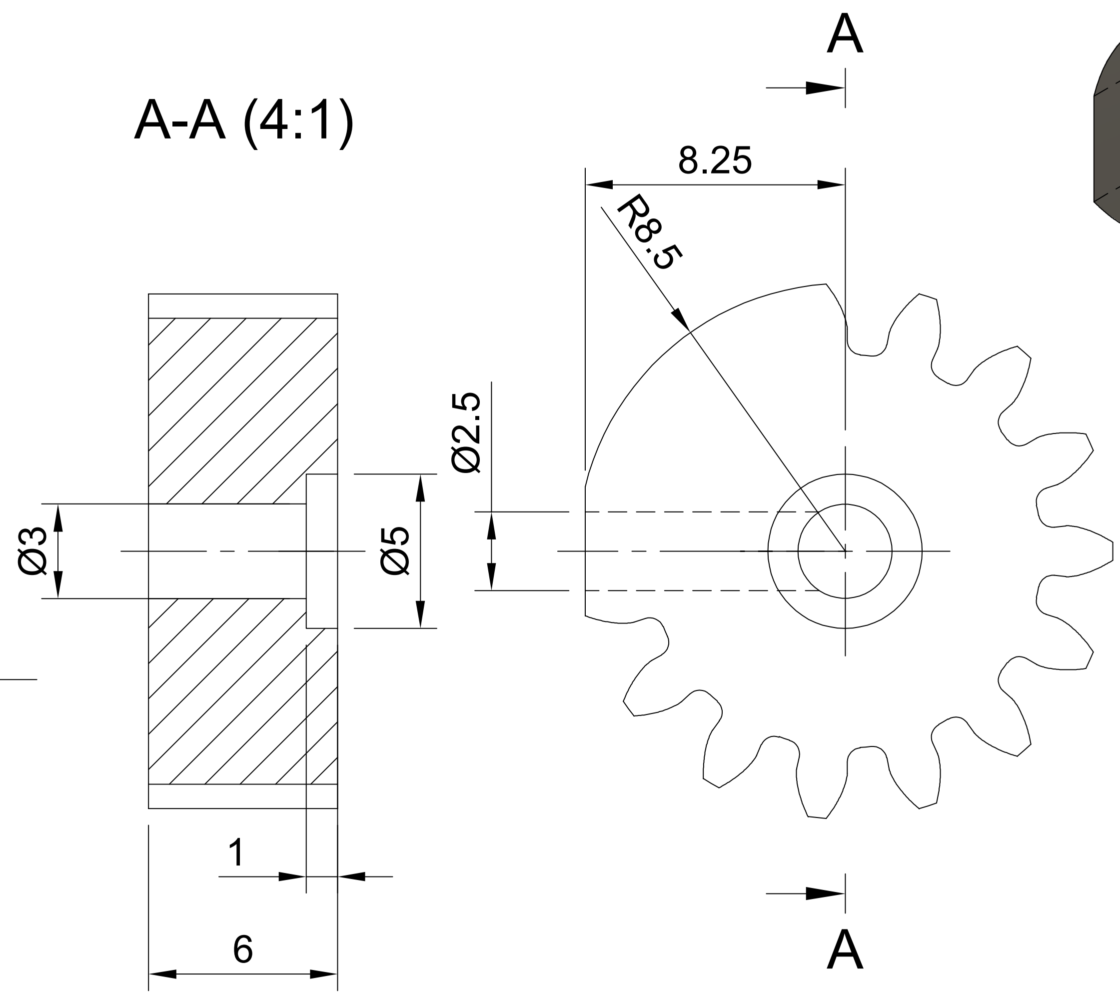


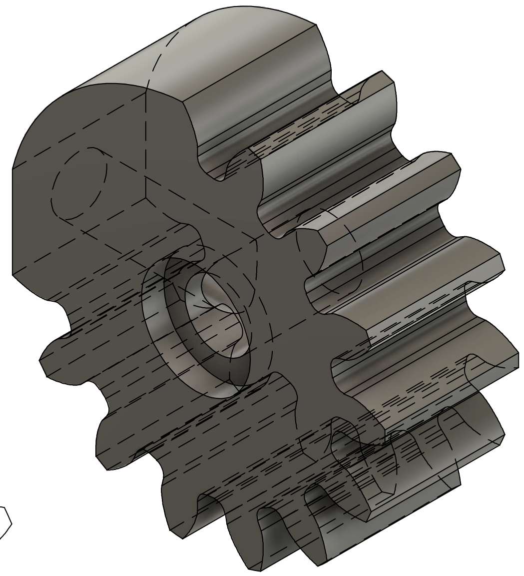

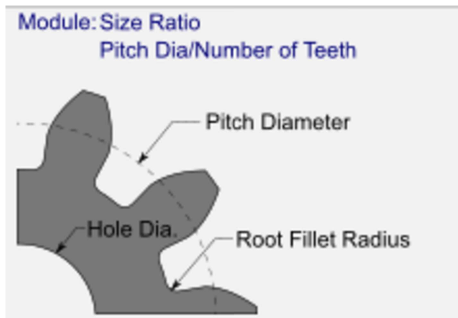


| | |
|---|---|
| Standard | Metric |
| Pressure Angle | 20 deg |
| Module | 1 |
| Number of Teeth | 15 |
| Backlash | 0.00 mm |
| Root Fillet Radius | 0.5 mm |
| Gear Thickness | 6 mm |
| Hole Diameter | 3.3 mm |
| Pitch Diameter | 15.00 mm |

| Dept. | Technical reference | Created by<br>Bram Van Riessen 01/09/2023 | Approved by |
|---|---|---|---|
| | | Document type<br>A4 | Document status |
| | | Title<br>Spur Gear (15 teeth)<br>Scale 4:1<br>Material: PLA | DWG No.<br>Rev. / Date of issue / Sheet 1/1 |

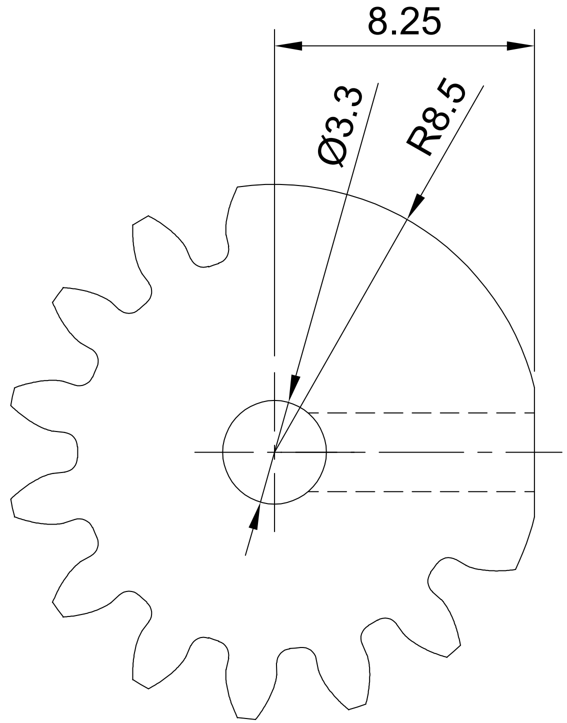


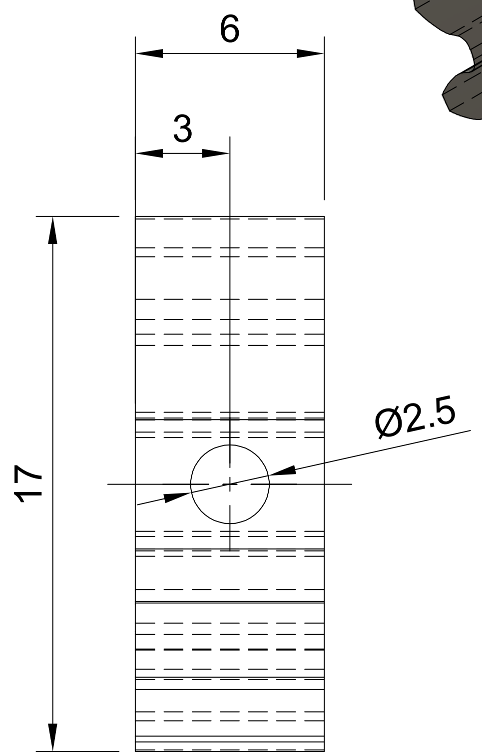


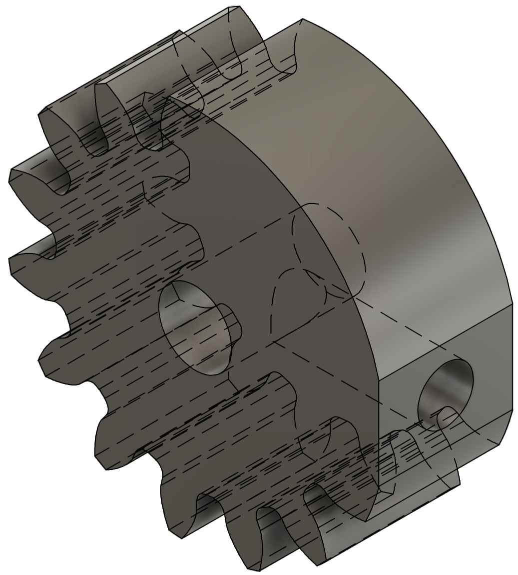

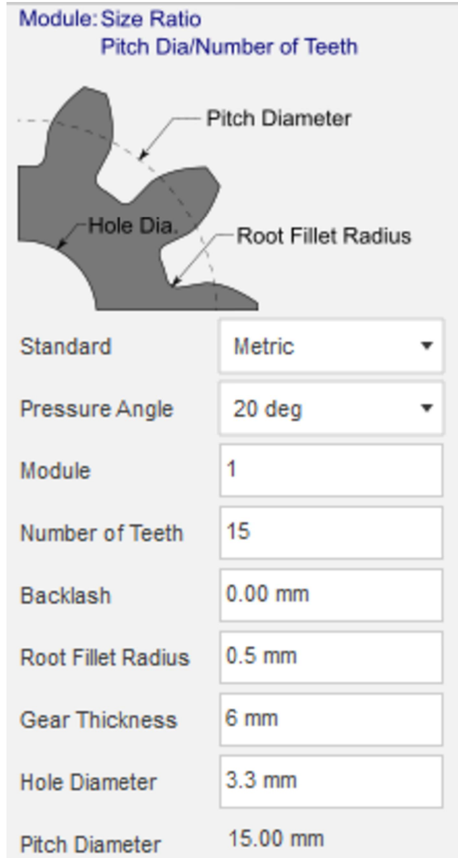


| | | | |
|---|---|---|---|
| Dept. | Technical reference | Created by<br>Bram Van Riessen 31/08/2023 | Approved by |
| | | Document type<br>A4 | Document status |
| | | Title<br>Spur Gear right (15 teeth)<br>Scale 4:1<br>Material: PLA | DWG No.<br>Rev. / Date of issue / Sheet 1/1 |

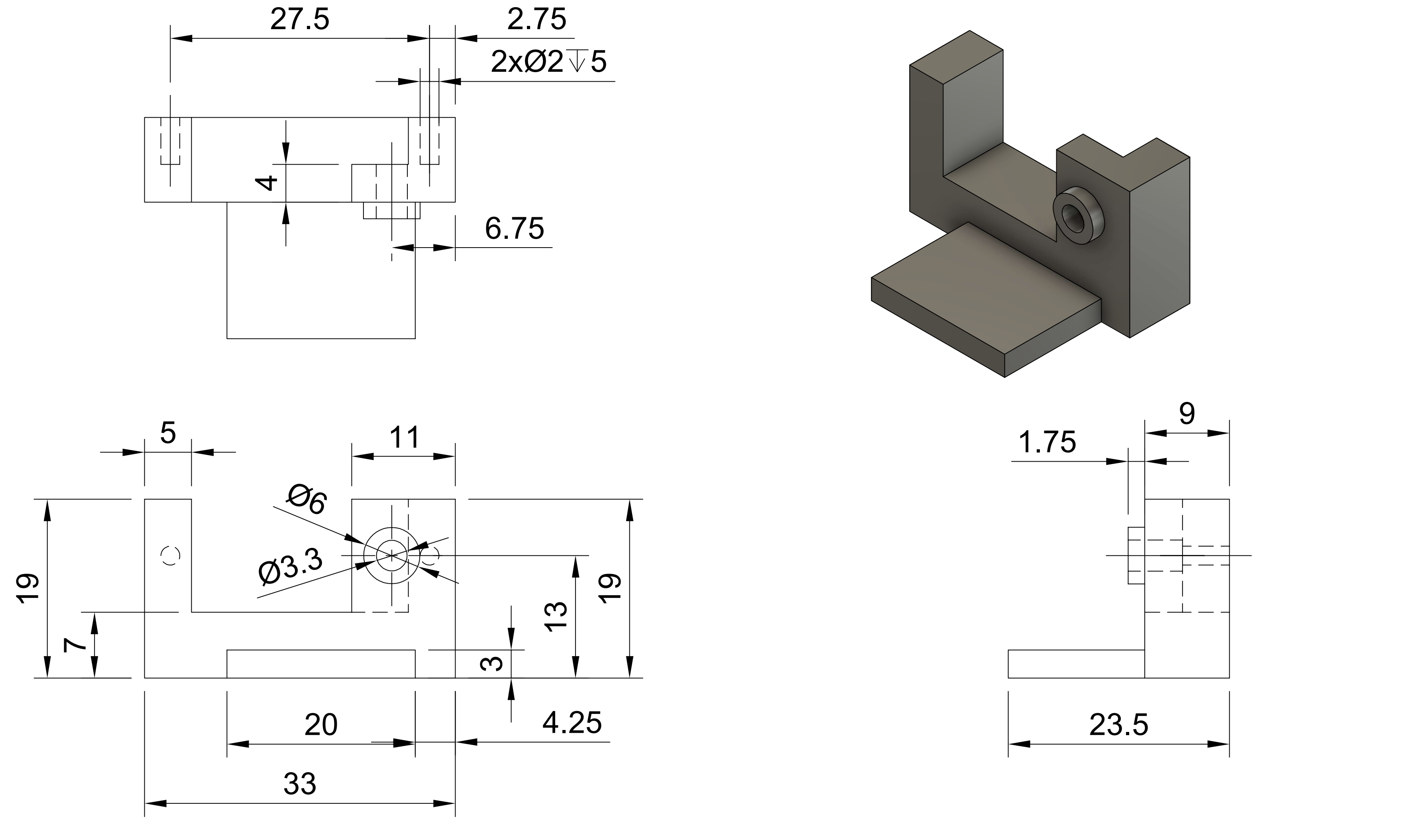


| Dept. | Technical reference | Created by | Approved by | | |
|---|---|---|---|---|---|
| | | Bram Van Riessen 31/08/2023 | | | |
| | | Document type: A4 | Document status | | |
| | | Title: MountingPlate-15teeth-spur<br>Scale 1.5:1<br>Material: PLA | DWG No. | | |
| | | | Rev. | Date of issue | Sheet 1/1 |

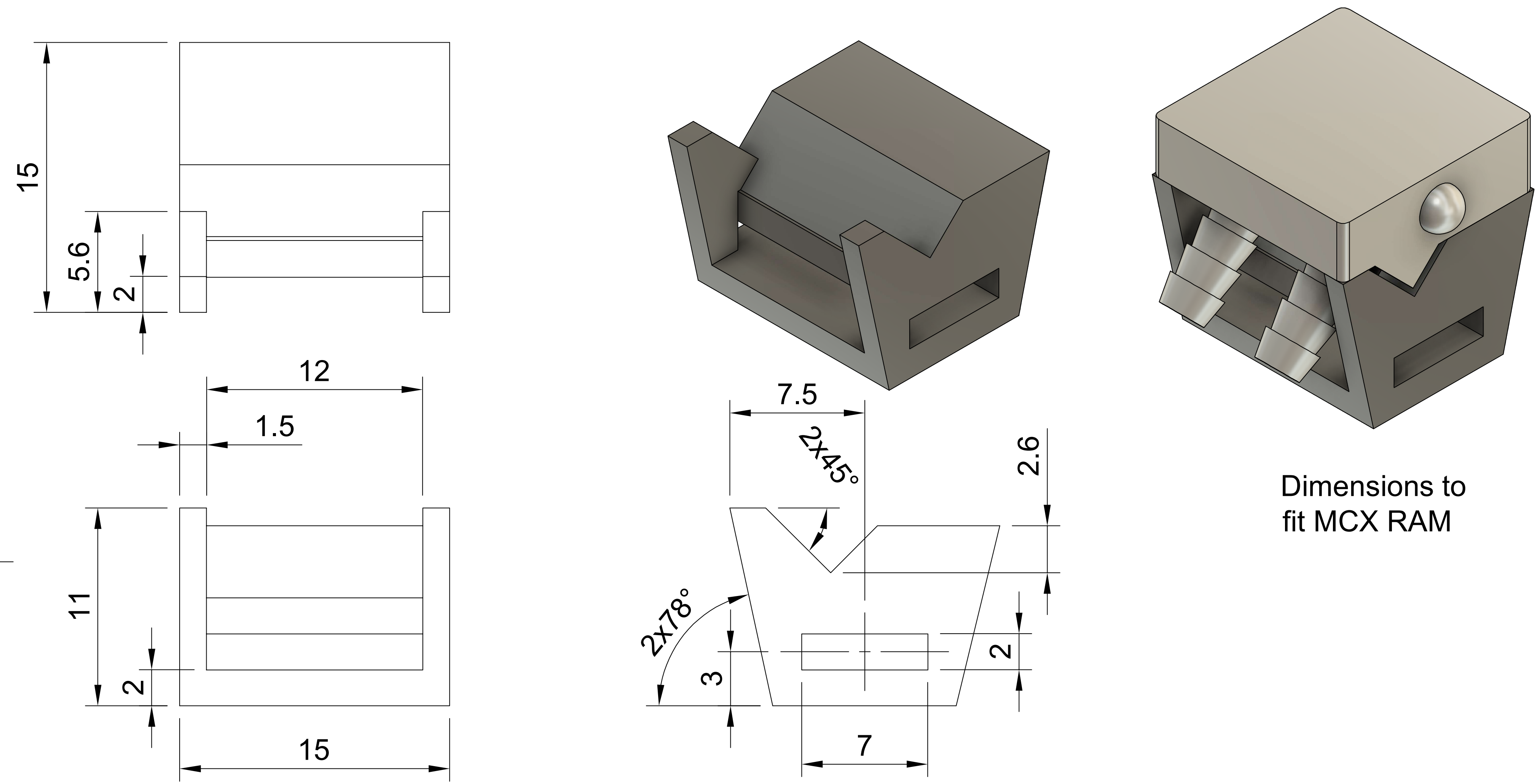


| Dept. | Technical reference | Created by | Approved by |
|---|---|---|---|
| | | Bram Van Riessen 31/08/2023 | |
| | | Document type: A4 | Document status |
| | | Title: MCXMount<br>Scale 3:1<br>Material: PLA | DWG No. |
| | | | Rev. / Date of issue / Sheet 1/1 |

# B

# Stimuli parameters and measurements

## B.1. Parameters

For the temperature values, the resistance of the NTC thermistor is calculated by using the voltage divider equation:

$$R_2 = R_1(\frac{V_i}{V_o} - 1.0) \tag{B.1}$$

where $R_2$ is the resistance of the thermistor, $R_1$ is the resistance of a known resistor, which is 10 kΩ in our case, $V_i$ is the input voltage and $V_o$ is the output voltage. After evaluating $R_2$, this value can be used to obtain the temperature by using the Steinhart-Hart equation [4]:

$$\frac{1}{T} = c_1 + c_2 \ln(R_2) + c_3 \ln(R_2)^3 \tag{B.2}$$

where $T$ is the temperature, and $c_1$, $c_2$, and $c_3$ are the Steinhart-Hart coefficients based on the resistance-temperature curve of the thermistor supplier. The parameters used for these formulas can be found in Table B.1. The temperature coming from these equations functions as feedback for the PID control. The Kp, Ki, and Kd values are specifically selected for a slow settling time, low overshoot, and low error. During preliminary experiments, the values were tuned to settle faster, but this sudden switch in temperature caused discomfort as the temperature targets approached the uncomfortable range. Therefore, the values are hand-tuned to give participants time to get used to changing thermal sensations. Measurements from the three target temperatures (18 °C for cold, 32 °C for neutral, and 40 °C for hot) can be found in Figure B.1.

**Table B.1:** Temperature control parameters

| Parameter | Value |
|---|---|
| Kp | 15 |
| Ki | 1 |
| Kd | 1 |
| c1 | 1.129371894e-03 |
| c2 | 2.340874207e-04 |
| c3 | 0.8782575527e-07 |

For pressure values, we use the average of three voltage measurements passing through the force-sensing resistor. For the 0.5 N low-pressure and 2 N high-pressure conditions, we used 50 g and 200 g weights, respectively. This corresponded to voltage readings of 2.6 V and 3.1 V, which are used as targets during the automatic pressure calibration. During pressure calibration, the motor angle changes by +1 angle increments during every time step based on the voltage reading from the force sensor until reaching the pressure target. Voltage readings during calibration can be found in Figure B.2.

## B.2. Measurements

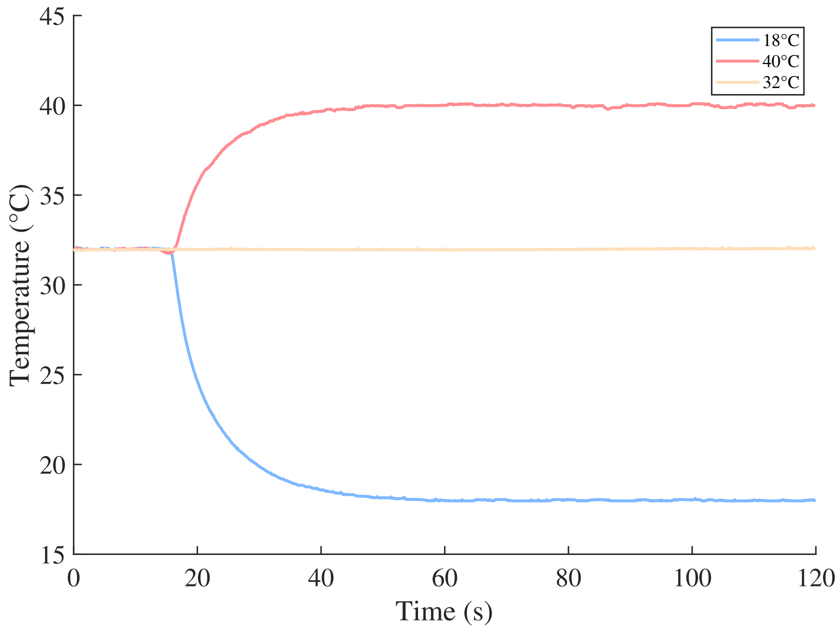


**Figure B.1:** Step response curves of the closed loop PID controlled temperature targets

**Table B.2:** Step response parameters. Step response after 15 seconds at 32 °C, settling time tolerance is 0.02.

| Target temperature (°C) | 18 | 32 | 40 |
|---|---|---|---|
| Settling time (s) | 41.6 | - | 39.80 |
| Overshoot (%) | -0.28 | - | +0.23 |
| Min error (°C) | -0.05 | -0.07 | -0.23 |
| Max error (°C) | +0.11 | +0.11 | +0.09 |

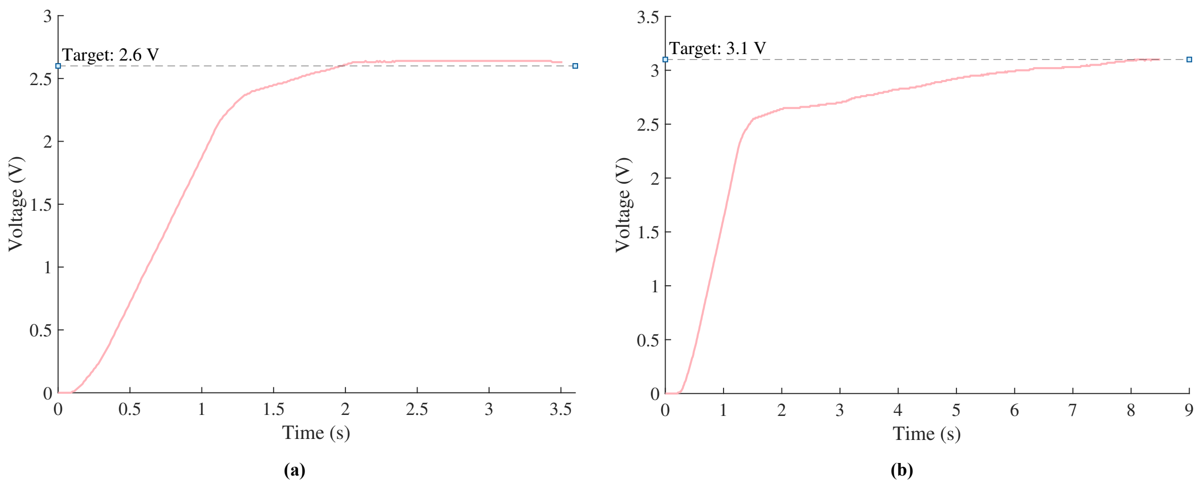


**Figure B.2:** Pressure calibration of (a) 0.5 N (2.6 V, settling time 3.52 s) and (b) 2 N (3.1 V, settling time 8.51 s) targets.

# C

# Pseudo code

Algorithm 1 shows the functionality of the ”VibrotactileSensitivity.mlapp” script based on a three-up/one-down adaptive staircase method. This method obtains thresholds with a correct response probability of 75% [5]. Algorithm 2 changes the amplitude based on answer correctness. Algorithm 3 checks if the last result is a reversal and if the last five reversals are within range to stop the trial.

**Algorithm 1** Main code of the vibratory threshold experiment

```
amplitude, oldAmplitude ← 20 mV
dBChange ← 5 dB
correctCounter ← 0
output ← amplitude · sin(2π · 250t)                  ▷ Vibration signal output
reversalValues ← [100 100 100 100 100]   ▷ Array of last 5 reversals, initialize with high values
differencePositive ← false                 ▷ Boolean for checking reversal direction
n ← 0                                      ▷ Number of reversals
for i = 80 do
    c ← randomInt(1 or 2)
    for j = 1 : 2 do                ▷ play two intervals of which one contains vibration
        soundcue(interval sound cue)
        pause(0.5 s)
        lamp(j, 'on')
        if c == j then
            write(output, 1 s)
        else
            pause(1 s)
        end if
        lamp(j, 'off')
    end for
    soundcue(question sound cue)
    QuestionLabel.Text ← '1 or 2?'
    waitforbuttonpress( )                  ▷ wait for answer from participant
    keyPressed ← 1 or 2, depending on the answer
    correctCheck( c, keyReturn, amplitude, correctCounter )
    output ← amplitude · sin(2π · 250t)
    reversalCheck( differencePositive, oldAmplitude, amplitude, reversalValues, n )
    oldAmplitude ← amplitude
    pause(0.5 s)
end for
```

**Algorithm 2** Changing the amplitude based on answer correctness

```
function correctCheck(c, keyReturn, amplitude, correctCounter)
    if c == keyReturn then
        QuestionLabel.Text ← 'Correct!'
        correctCounter ← correctCounter + 1
        if correctCounter == 3 then                          ▷ Decrease amplitude after 3 correct answers
            amplitude ← amplitude/10^(dBChange/20)
            correctCounter ← 0
        end if
    else
        QuestionLabel.Text ← 'Incorrect'                     ▷ Increase amplitude after 1 incorrect answers
        amplitude ← amplitude · 10^(dBChange/20)
    end if
    return amplitude                                         ▷ Return the changed amplitude
end function
```

**Algorithm 3** Check last 5 reversals and stop trial if within range

```
function reversalCheck(differencePositive, oldAmplitude, amplitude, reversalValues, n)
    if differencePositive then
        if oldAmplitude > amplitude then
            reversalCondition ← true
            differencePositive ← false
        end if
    else
        if oldAmplitude < amplitude then
            reversalCondition ← true
            differencePositive ← true
        end if
    end if
    if reversalCondition then
        n ← n + 1
        reversalValues[end] ← oldAmplitude
        reversalDifference ← 20 · log10(max(reversalValues)/ min(reversalValues))
        if reversalDifference ≤ 2 then
            break
        end if
        reversalValues ← circshift(reversalValues, 1)        ▷ shift reversal entries one space
        reversalCondition ← false                            ▷ reset reversal condition
        intensityIncrement ← 1dB                             ▷ change increment to 1 dB after first reversal
    end if
end function
```

# D

# Additional data insights

An overview of the main results is shown in Table D.1, accompanied by the per participant vibratory detection thresholds given in Figure D.1.

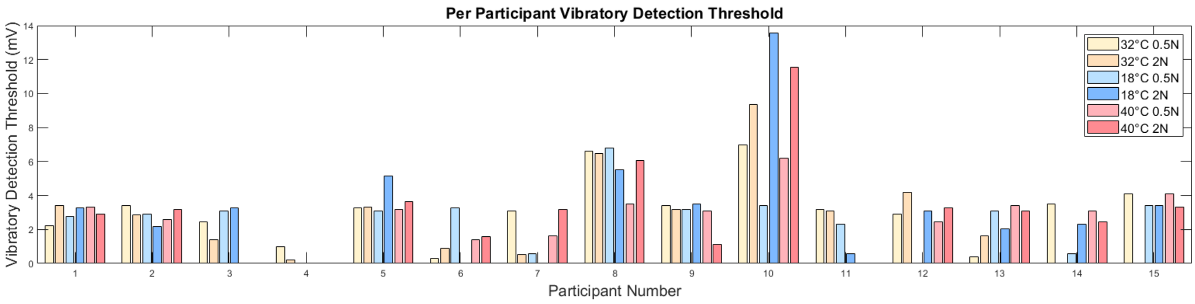


**Figure D.1:** Vibratory detection thresholds per participant.

**Table D.1:** Vibratory Detection Thresholds (mV)

| Condition | Data points | Min | Max | Mean | SD |
|---|---|---|---|---|---|
| 18 °C 0.5 N | 13 | 0.58 | 6.79 | 2.96 | 1.50 |
| 18 °C 2 N | 12 | 0.59 | 13.54 | 3.99 | 3.29 |
| 32 °C 0.5 N | 15 | 0.30 | 6.96 | 3.12 | 1.88 |
| 32 °C 2 N | 13 | 0.23 | 9.37 | 3.12 | 2.54 |
| 40 °C 0.5 N | 12 | 1.39 | 6.20 | 3.17 | 1.23 |
| 40 °C 2 N | 12 | 1.13 | 11.55 | 3.78 | 2.73 |

Since every participant converged for the neutral thresholds, the other conditions can be compared with the neutral condition results by calculating the dB difference (see Figure D.2a).

$$dB = 20log10(\frac{V_{neutral}}{V_{other}}) \tag{D.1}$$

In Figure D.2a, it can be seen that boxplots of pressure conditions are shifted downwards slightly, indicating the sensitivity decrease caused by relocated pressure. However, the boxplots are strikingly similar, and no consistent dB increase or decrease compared to the neutral condition can be found.

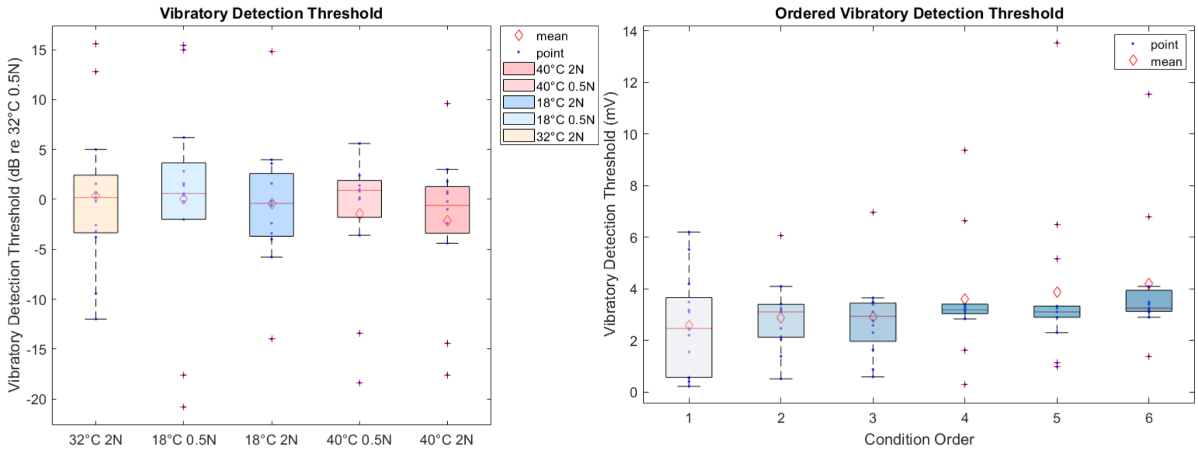


**(a)** **(b)**

**Figure D.2:** (a) Boxplot of comparing neutral condition with 5 other conditions (see Table D.2 for numeric display of data)and (b) results of vibratory detection thresholds depending on condition order (see Table D.3 for numeric display of data).

**Table D.2:** Vibratory Detection Thresholds compared to neutral conditions (dB re 32 C 0.5 N)

| Condition | Min | LA | Mean | UA | Max |
|---|---|---|---|---|---|
| 32 °C 2 N | -12.00 | -12.00 | 0.37 | 5.00 | 15.60 |
| 18 °C 0.5 N | -20.82 | -2.00 | 0.06 | 6.20 | 15.42 |
| 18 °C 2 N | -14.00 | -5.78 | -0.40 | 3.98 | 14.81 |
| 40 °C 0.5 N | -18.38 | -3.60 | -1.45 | 5.60 | 5.60 |
| 40 °C 2 N | -17.60 | -4.40 | -2.11 | 3.00 | 9.59 |

**Table D.3:** Vibratory Detection Thresholds (mV) depending on Condition Order

| Order | Data points | Min | Max | Mean | SD |
|---|---|---|---|---|---|
| 1 | 13 | 0.23 | 6.20 | 2.59 | 1.95 |
| 2 | 13 | 0.52 | 6.07 | 2.89 | 1.35 |
| 3 | 12 | 0.59 | 6.96 | 2.90 | 1.64 |
| 4 | 13 | 0.30 | 9.37 | 3.60 | 2.22 |
| 5 | 15 | 0.98 | 13.54 | 3.86 | 2.99 |
| 6 | 11 | 1.39 | 11.55 | 4.21 | 2.75 |

To evaluate the effect of exhaustion based on the order of the condition sequence, the threshold results are combined in a boxplot (see Figure D.2b). The minimum threshold value per condition is lowest overall for the first condition and highest for the last condition. Moreover, the maximum threshold values are the highest for the last three conditions. It must be noted that these three values all come from the same participant, and excluding these outliers results in comparable boxplots for the six conditions. Nonetheless, these results show that participants can focus better when they start the experiment, and this ability to focus reduces slightly afterward. Even though participants had breaks of 10 minutes between conditions, mental fatigue did play a minor role in the execution of the experiment.

# E

# Safety and Ethics

Participant safety is crucial, which is why the Human Research Ethics Committee of TU Delft is involved in experiments featuring participants.

As our multimodal haptic ring is custom-designed, the author made a device report that goes over the design of non-CE-certified devices and includes a risk analysis with potential hazards and corresponding mitigation measures. The 3mE safety advisor evaluated this device and the device report to ensure participants' safety.

Informed consent prepares the participant to know what is coming and ensures that the participant agrees to the conditions of the experiment. Every participant had to fill in the informed consent form after the experimenter gave a presentation about experimental procedures so they knew what was involved. This form is the only document containing the participants' names; all collected data is anonymized.

Furthermore, the author created a data management plan to ensure participants' privacy by stating how collected data and personal information are stored. Also, an HREC checklist ensures the submission is complete and all essential processes are considered. This data management plan and HREC checklist are not included in the appendices but can be found in the Human Research Ethics Committee database with case number 3279, as the submission was approved.

# Delft University of Technology
# INSPECTION REPORT FOR DEVICES TO BE USED IN CONNECTION WITH HUMAN SUBJECT RESEARCH

This report should be completed for every experimental device that is to be used in interaction with humans and that is not CE certified or used in a setting where the CE certification no longer applies[1].

The first part of the report has to be completed by the researcher and/or a responsible technician.

Then, the safety officer (Heath, Security and Environment advisor) of the faculty responsible for the device has to inspect the device and fill in the second part of this form. An actual list of safety-officers is provided on this webpage.

Note that in addition to this, all experiments that involve human subjects have to be approved by the Human Research Ethics Committee of TU Delft. Information on ethics topics, including the application process, is provided on the HREC website.

**Device identification (name, location):** Multimodal Haptic Ring, (CoR lab, F-0-470)

**Configurations inspected[2]: NA**

**Type of experiment to be carried out on the device:[3]** Vibrotactile sensitivity experiment - Applying thermal and pressure cues to the finger connection (proximal phalanx) while applying vibrotactile cues to the fingertip (distal phalanx)

**Name(s) of applicants(s):** Dr. Y. (Yasemin) Vardar and H.A.J. (Bram) van Riessen

**Job title(s) of applicants(s):** Assistant Professor and Master's student

(Please note that the inspection report should be filled in by a TU Delft employee. In case of a BSc/MSc thesis project, the responsible supervisor has to fill in and sign the inspection report.)

**Date:** 12.06.2023

**Signature(s):** Yasemin Vardar

Yasemin Vardar

1 Modified, altered, used for a purpose not reasonably foreseen in the CE certification

2 If the devices can be used in multiple configurations, otherwise insert NA

3 e.g. driving, flying, VR navigation, physical exercise, ...

## Setup summary

*Please provide a brief description of the experimental device (functions and components) and the setup in which context it supposed to be used. Please document with pictures where necessary.*

*More elaborate descriptions should be added as an appendix (see below).*

The multimodal haptic ring can apply thermal and pressure cues to the connection of the finger (proximal phalanx). For the thermal cues, a 15x15x3.6 mm Peltier module (QC-31-1.0-3.9AS, QuickCool) is used to apply warm or cold temperatures to the finger. A PID-controlled motor driver (DRV8833, Pololu) regulates the current to maintain the target temperatures, which obtains temperature feedback through the thermistor (GA10K3MCD1 NTC Thermistor, TE Connectivity) that is placed on the Peltier module. This module is placed on a water-cooled heat sink (MCX RAM, Alphacool) for heat dissipation. A water pump (Centrifugal Water Pump 480-122, RS Pro) circulates the water through the heat sink with silicon hoses for feeding the water.

This assembly is placed on a moving 3D-printed mount, which is connected to a GT2-6 belt. The two ends of the belt are connected to 3D-printed spur gears. The spur gears move in opposite directions, making the platform move either up or down driven by the MG90S servo motor. This servo motor is connected to a 3D-printed mount, which contains a force-sensing resistor (FSR06B, Ohmite) to indicate the applied pressure.

‘The fingertip has a separate haptic ring for vibrotactile cues applied by a voice coil actuator (Haptuator Mark II, Tactile Labs). A NI-DAQ (PCIe-6363, NI) outputs a sinusoidal signal amplified by an audio amplifier (MIKROE-3077, Mikroe) which causes vibrotactile cues when connected to the voice coil actuator. The voice coil actuator is mounted on a velcro strap, connected to an acrylic plate that contains a force-sensing resistor (FSR06B, Ohmite) for evaluating the attachment force.

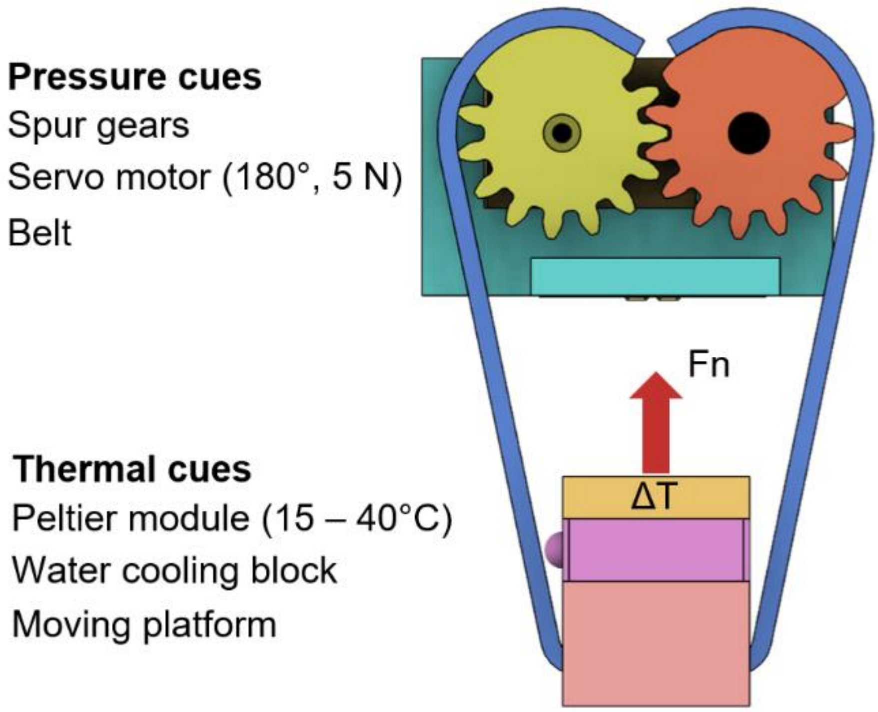

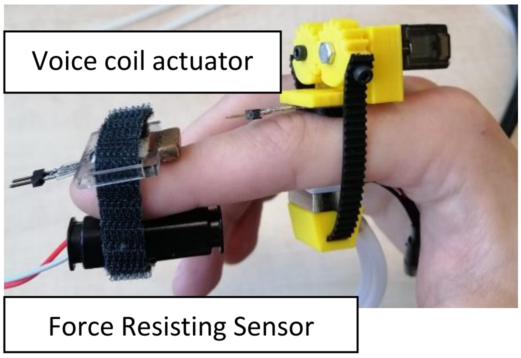
Voice coil actuator
Force Resisting Sensor


Force Resisting Sensor

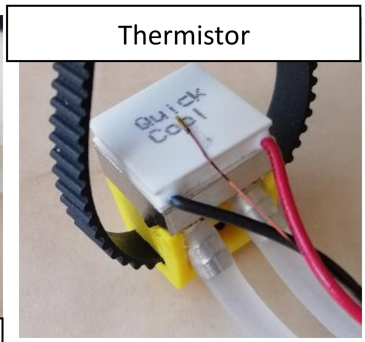
Thermistor
Quick Cool

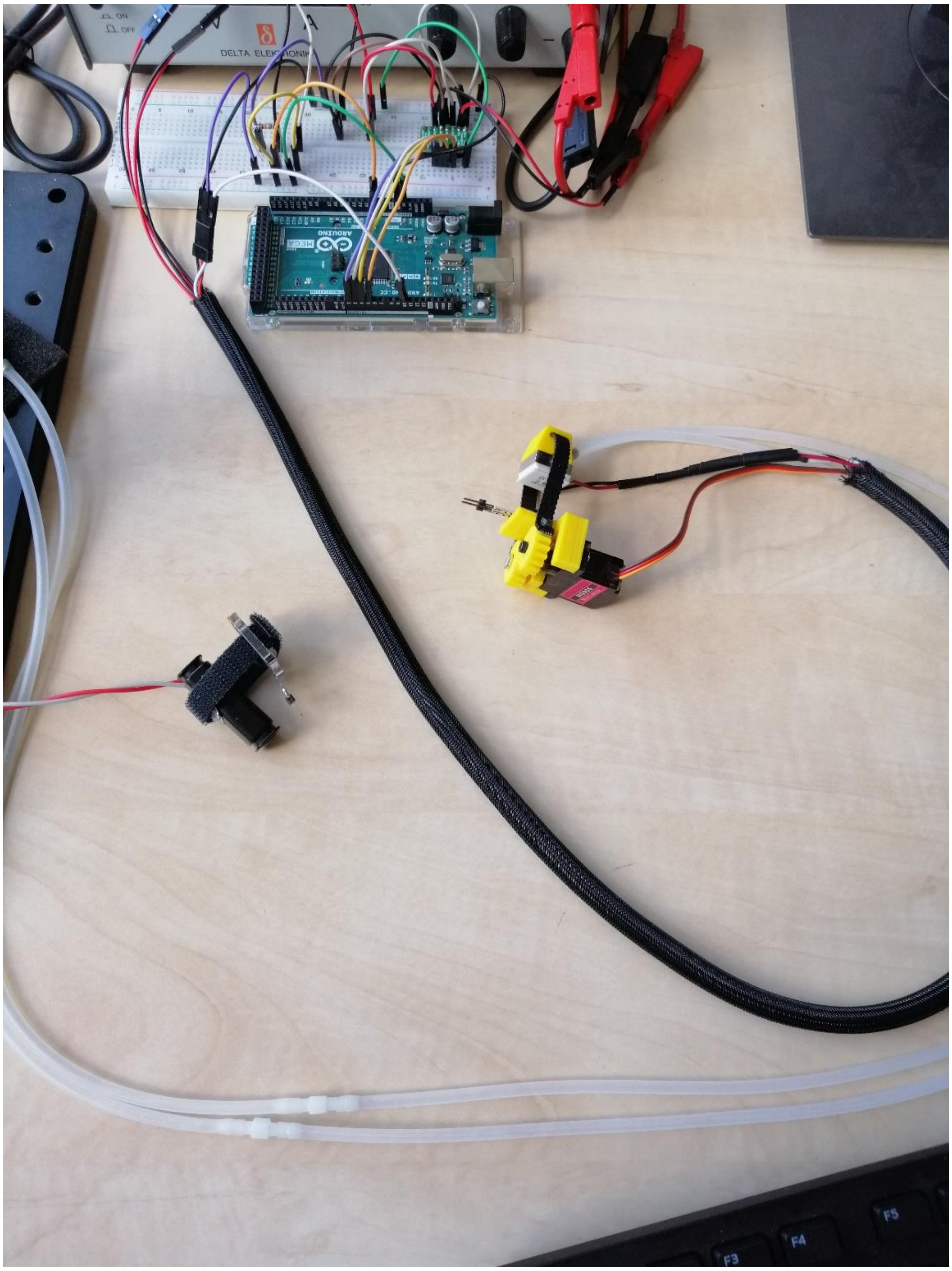

**Risk checklist**

Please fill in the following checklist and consider these hazards that are typically present in many research setups. If a hazard is present, please describe how it is dealt with.

Also, mention any other hazards that are present.

| **Hazard type** | **Present** | **Hazard source** | **Mitigation measures** |
|---|---|---|---|
| Mechanical (sharp edges, moving equipment, etc.) | Yes | Voice coil actuator for vibrotactile cues<br><br>Servo motor driven belt for pressure cues | The amplifier that drives the actuator has a 12VDC power supply, the signal cannot go past this. During the experiment, the voltage will be < 1VDC as the signal should be barely perceivable.<br><br>The servo motor can apply a maximum force of 1.8 kg. During experiments, the force applied will be 500 grams or less. |
| Electrical | Yes | Wiring | The wires near the hand are fully insulated. |
| Structural failure | Yes | Servo motor driven belt for pressure cues | The attached spur gears could get detached over time or the gears could get worn out over long periods of usage, but this will result in a decrease in pressure which is not harmful to participants. |
| Touch Temperature | Yes | Peltier module for thermal cues | The Peltier module is limited to 0.7 A to slowly increase and decrease the temperature to max. 40 °C and min. 15 °C. This range is within the comfortable non-painful range of humans. |
| Electromagnetic radiation | No | | |
| Ionizing radiation | No | | |
| (Near-)optical radiation (lasers, IR-, UV-, bright visible light sources) | No | | |
| Noise exposure | No | | |
| Materials (flammability, offgassing, etc.) | No | | |
| Chemical processes | No | | |
| Fall risk | No | | |
| *Other:* | | | |
| *Other:* | | | |
| *Other:* | | | |

## Device inspection

(to be filled in by the AMA advisor of the corresponding faculty)

**Name:** Peter Kohne

**Faculty:** 3mE-IO

The device and its surroundings described above have been inspected. During this inspection I could not detect any extraordinary risks.

*(Briefly describe what components have been inspected and to what extent (i.e. visually, mechanical testing, measurements for electrical safety etc.)*

**Date:** 12-06-2023

**Signature:**

Inspection valid until[4]:

Note: changes to the device or set-up, or use of the device for an experiment type that it was not inspected for require a renewed inspection

4 Indicate validity of the inspection, with a maximum of 3 years

**Delft University of Technology**
**HUMAN RESEARCH ETHICS**
**EXPLICIT CONSENT**

| PLEASE TICK THE APPROPRIATE BOXES | Yes | No |
|---|---|---|
| **A: GENERAL AGREEMENT – RESEARCH GOALS, PARTICPANT TASKS AND VOLUNTARY PARTICIPATION** | | |
| 1. I have read and understood the study information dated [*DD/MM/YYYY*], or it has been read to me. I have been able to ask questions about the study and my questions have been answered to my satisfaction. | ☐ | ☐ |
| 2. I consent voluntarily to be a participant in this study and understand that I can refuse to answer questions and I can withdraw from the study at any time, without having to give a reason. | ☐ | ☐ |
| 3. I understand that taking part in the study involves:<br>• Evaluating when a vibrotactile signal is applied to the best of my ability | ☐ | ☐ |
| 4. I understand that I will not be compensated for my participation | ☐ | ☐ |
| 5. I understand that the study will end when the master thesis period is completed | ☐ | ☐ |
| **B: POTENTIAL RISKS OF PARTICIPATING (INCLUDING DATA PROTECTION)** | | |
| 6. I understand that taking part in the study involves the following risks:<br>• Being exposed to harmless cold and warm thermal stimuli which could be perceived as uncomfortable or painful<br>• Being exposed to harmless pressure stimuli which could be perceived as uncomfortable or painful<br>• Being exposed to harmless vibrotactile stimuli which could be perceived as uncomfortable or painful<br>I understand that these will be mitigated by:<br>• Device inspection performed by the faculty HSE advisor, who prevents unnecessary risks during the use of the device<br>• Keeping the stimuli within the non-painful range | ☐ | ☐ |
| 7. I understand that taking part in the study also involves collecting specific personally identifiable information (PII) such as my name, age, sex, and contact informationwith the potential risk of my identity being revealed in the case of a data breach. No personally identifiable research data (PIRD) will be collected | ☐ | ☐ |
| 9. I understand that the following steps will be taken to minimise the threat of a data breach, and protect my identity in the event of such a breach:<br>• Keeping the link to the data and my identity in a locked cabinet only during the experimental period where the corresponding and responsible researchers can reach it<br>• Destroying the link to my identity after the experiments period (pseudoanonymisation)<br>• Not stating my name when the data is published | ☐ | ☐ |
| 10. I understand that personal information collected about me that can identify me, such as my name, will not be shared beyond the study team. | ☐ | ☐ |

| PLEASE TICK THE APPROPRIATE BOXES | Yes | No |
|---|---|---|
| 11. I understand that the (identifiable) personal data I provide will be destroyed after the thesis period | ☐ | ☐ |
| **C: RESEARCH PUBLICATION, DISSEMINATION AND APPLICATION** | | |
| 12. I understand that after the research study the de-identified information I provide will be used for comparing conditions in the corresponding researcher's master thesis, with the aim to publish this research. | ☐ | ☐ |
| 13. I agree that my responses, views or other input can be quoted anonymously in research outputs | ☐ | ☐ |
| **D: (LONGTERM) DATA STORAGE, ACCESS AND REUSE** | | |
| 16. I give permission for the de-identified age, sex, and vibrotactile sensitivity thresholds that I provide to be archived in 4TU.ResearchData repository so it can be used for future research and learning. | ☐ | ☐ |
| 17. I understand that access to this repository is open. | ☐ | ☐ |

**Signatures**

| ____________________________ | ___________________________ | _________ |
|---|---|---|
| Name of participant [printed] | Signature | Date |

I, as researcher, have accurately read out the information sheet to the potential participant and, to the best of my ability, ensured that the participant understands to what they are freely consenting.

| __________________________ | ____________________ | _________ |
|---|---|---|
| Researcher name [printed] | Signature | Date |

Study contact details for further information: [*Name, phone number, email address*]

H.A.J. van Riessen, +31641540531, h.a.j.vanriessen@student.tudelft.nl

# References


[1] Massimiliano Gabardi et al. "Development of a miniaturized thermal module designed for integration in a wearable haptic device". In: *2018 IEEE Haptics Symposium (HAPTICS)*. IEEE. 2018, pp. 100–105.

[2] Hsin-Ni Ho and Lynette A Jones. "Modeling the thermal responses of the skin surface during hand-object interactions". In: (2008).

[3] Lynette A Jones and Hsin-Ni Ho. "Warm or cool, large or small? The challenge of thermal displays". In: *IEEE Transactions on Haptics* 1.1 (2008), pp. 53–70.

[4] John S Steinhart and Stanley R Hart. "Calibration curves for thermistors". In: *Deep sea research and oceanographic abstracts*. Vol. 15. 4. Elsevier. 1968, pp. 497–503.

[5] Jozef J Zwislocki and Evan M Relkin. "On a psychophysical transformed-rule up and down method converging on a 75% level of correct responses". In: *Proceedings of the National Academy of Sciences* 98.8 (2001), pp. 4811–4814.